BEST AVAILABLE IMAGES

Defective images within this document are accurate representations of the original documents submitted by the applicant.

Defects in the images may include (but are not limited to):

- BLACK BORDERS
- TEXT CUT OFF AT TOP, BOTTOM OR SIDES
- FADED TEXT
- BLURRY OR ILLEGIBLE TEXT
- SKEWED/SLATED IMAGES
- COLORED PHOTOS
- BLACK OR VERY DARK BLACK AND WHITE PHOTOS
- UNDECIPHERABLE GRAY SCALE DOCUMENTS

IMAGES ARE BEST AVAILABLE COPY.

As rescanning documents *will not* correct images, please do not report the images to the Image Problem Mailbox.

INTERNATIONAL APPLICATION PUBLISHED UNDER THE PATENT COOPERATION TREATY (PCT)

(51) International Patent Classification 5 : G21B 1/00 — A1

(11) International Publication Number: WO 93/01601

(43) International Publication Date: 21 January 1993 (21.01.93)

(21) International Application Number: PCT/US92/05717

(22) International Filing Date: 8 July 1992 (08.07.92)

(30) Priority data:

727,275	11 July 1991 (11.07.91)	US
758,869	11 September 1991 (11.09.91)	US
792,205	12 November 1991 (12.11.91)	US

(71) Applicant: UNIVERSITY OF UTAH RESEARCH FOUNDATION [US/US]; 210 Park Building, Salt Lake City, UT 84112 (US).

(72) Inventors: CEDZYNSKA, Krystyna ; ul. Zgierska 75/81, 91-464 Lodz (PL). LINTON, Denton, C. ; 2845 Bonnie Brae, Salt Lake City, UT 84124 (US). WILL, Fritz, G. ; 348 Lake Shore Road, P.O. Box 705, Willsboro, NY 12993 (US).

(74) Agent: PRAHL, Eric, L.; Fish & Richardson, 225 Franklin Street, Boston, MA 02110-2804 (US).

(81) Designated States: BR, CA, JP, RU, European patent (AT, BE, CH, DE, DK, ES, FR, GB, GR, IT, LU, MC, NL, SE).

Published

With international search report.

Before the expiration of the time limit for amending the claims and to be republished in the event of the receipt of amendments.

(54) Title: METHOD FOR CONSISTENT REPRODUCTION OF HIGH DEUTERIUM LOADING AND TRITIUM GENERATION IN PALLADIUM ELECTRODES

(57) Abstract

Isotopic hydrogen is electrolytically loaded into a palladium or palladium alloy electrode (22) by alternately charging and discharging the electrode in a plurality of cycles, each cycle including charging the electrode with isotopic hydrogen approximately to a saturation level and then discharging the electrode to a predetermined retention level. The electrode can be palladized by electrodeposition of a thin coating of Pd black, then pre-loaded in deuterium gas at atmospheric pressure, then transferred to an electrochemical cell (20) where the alternate charging and discharging takes place for a total of 4-5 times.

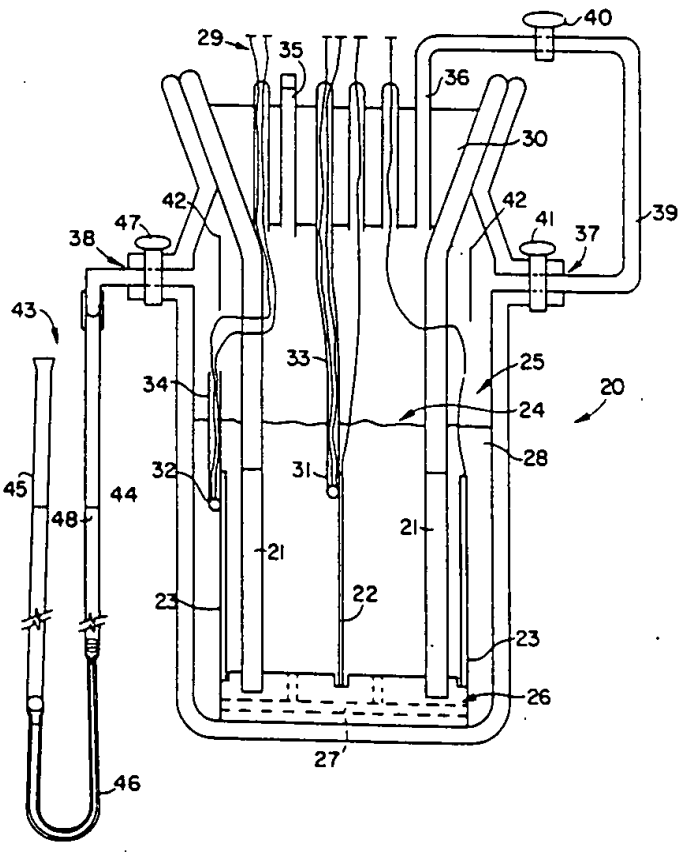

p.10, P37 sulfuric acid

FOR THE PURPOSES OF INFORMATION ONLY

Codes used to identify States party to the PCT on the front pages of pamphlets publishing international applications under the PCT.

AT	Austria	FI	Finland	ML	Mali
AU	Australia	FR	France	MN	Mongolia
BB	Barbados	GA	Gabon	MR	Mauritania
BE	Belgium	GB	United Kingdom	MW	Malawi
BF	Burkina Faso	GN	Guinea	NL	Netherlands
BG	Bulgaria	GR	Greece	NO	Norway
BJ	Benin	HU	Hungary	PL	Poland
BR	Brazil	IE	Ireland	RO	Romania
CA	Canada	IT	Italy	RU	Russian Federation
CF	Central African Republic	JP	Japan	SD	Sudan
CG	Congo	KP	Democratic People's Republic of Korea	SE	Sweden
CH	Switzerland			SN	Senegal
CI	Côte d'Ivoire	KR	Republic of Korea	SU	Soviet Union
CM	Cameroon	LI	Liechtenstein	TD	Chad
CS	Czechoslovakia	LK	Sri Lanka	TG	Togo
DE	Germany	LU	Luxembourg	US	United States of America
DK	Denmark	MC	Monaco		
ES	Spain	MG	Madagascar		

METHOD FOR CONSISTENT REPRODUCTION OF HIGH DEUTERIUM LOADING AND TRITIUM GENERATION IN PALLADIUM ELECTRODES

Background of the Invention

Technical Field.

The present invention relates generally to the diffusion of isotopic hydrogen into hydrogen-absorbing electrodes, and more particularly to a method for consistently achieving a high loading ratio of isotopic hydrogen in hydrogen absorbing electrodes. Specifically, the present invention relates to a method that has consistently achieved a sufficiently high deuterium loading ratio in palladium electrodes that the generation of tritium has been consistently observed.

Background Art.

It is well known that palladium may absorb large quantities of hydrogen and its isotopes. Upon absorption, two phases are formed, known as the a-phase and the b-phase, in which the palladium hydride PdH_n or deuteride PdD_n are formed. Moreover, the study of absorption of isotopic hydrogen in palladium electrodes has been the subject of considerable work over the years. In general, consistent results have not been easily obtained.

T. Flanagan & F. Lewis, "Hydrogen Absorption by Palladium in Aqueous Solution," Transactions of the Faraday Society, Vol. 55, Part 8, August 1959, pp. 1400-1408, for example, disclose various pretreatments of palladium prior to measuring hydrogen absorption by the palladium in aqueous solution. As disclosed on page 1400, these pretreatments are said to include annealing at various temperatures, mechanical deformation and preliminary glow discharge in argon. Moreover, despite such treatments, it was found difficult to obtain reproducible rates of absorption.

Fedorova & T. Rzhischeva, "The Formation and

Stability of the B-Phase System of Palladium and Hydrogen in Aqueous Solution," Russian Journal of Physical Chemistry, Vol. 34, No. 3, March 1960, pp. 325-326, describes the preparation of palladium electrodes for experiments on the saturation of electrodes immersed in a solution with hydrogen. Before the experiment the electrodes were degreased by heating to 60°C in concentrated sulfuric acid, carefully washed in twice distilled water, anodically polarized for an hour in normal sulfuric acid, and then cathodically in a fresh solution of acid until the evolution of gas was noticed with the current at 0.002 A. In another experiment a palladium foil electrode was treated by washing in hot concentrated nitric acid, then washing it in twice-distilled water, and then heating it to white heat in air. After this the electrode was immersed in a normal solution of sulfuric acid, anodically polarized at 0.0002 A until its potential with the current flowing assumed a value of about 1 V, and then saturated with hydrogen, the potential and time being measured. This method of preliminary treatment of the electrode, with the complete exclusion of cathodic polarization, was said to give an electrode of low activity, the deactivation of the electrode being variable according to the duration and intensity of the heating, and apparently palladium electrodes sufficiently active with respect to the absorption and evolution of hydrogen can be made only by alternate anodic and cathodic polarization.

F. A. Lewis, "The Hydrided Palladium Electrode," Platinum Metals Review, Vol. 6, No. 1, January 1962, pp. 22-27, describes on page 23 the kinetics of absorption of hydrogen dissolved in solution by a catalytically active palladium wire, and the effect of poisoning of the catalytic surface. It is said that the results shown in FIG. 1 (on page 24 of the Lewis reference) may be excellently reproduced if the surface is activated by

palladization, but virtually identical results can be obtained with "bright" surfaces activated either by anodization or even merely by pre-flaming. However, the catalytic activity of pre-flamed or pre-anodized specimens is more readily negatived by poisons. Poisonous species can be present in either insufficiently purified electrolytes or in the hydrogen or other gas streams or be leached from the electrolyte container or specimen holder. There is also the possibility of copper, zinc or mercury being introduced into the electrolyte from electrical connections. It is further said that despite the elimination of catalytic poisons from the sources listed, extremely misleading data can be obtained if specimens are not efficiently cleaned before introduction into solution since subsequent activation procedures, such as anodization or cathodization, may not thereafter be entirely successful.

J. Barton and F. Lewis, "Determination of the Hydrogen Content of Palladium and Palladium Alloys from Measurement of Electrode Potential and Electrical Resistance," Talanta, Vol. 10 (1963), pp. 237-246, describes on page 239 a method of preparing electrodes to obtain sensible E-H/Pd relationships. It is said that it is necessary to prevent platinum, and other metal electrical leads to the specimen, from contacting the electrolyte. There is also much evidence to suggest that the electrode surface should be so catalytically active that the kinetics of equilibration with hydrogen molecules are governed, in vigorously stirred solutions, by the rate of diffusion of the molecules through the Brunner-Nernst layer, i.,e., by transport of the dissolved molecules up to, or away from, the surface of the electrode. Although the mechanism of activation is not fully understood, electrodes in the "bright" state which fulfill this latter condition have been prepared by preflaming and/or

anodization. However, fairly rigid conditions of purity of both hydrogen gas and electrolyte must then apply throughout the experiments in order to maintain a high catalytic activity. An electrode surface that is much less readily poisoned may be obtained by "palladizing", i-,e-, by plating the palladium (or palladium alloy) with a layer of palladium black from a dilute solution of chloropalladous acid (e.g., 2% $PdCl_2$ in 0.1N HCl).

More recently the study of the absorption and diffusion of hydrogen in palladium electrodes has been of renewed interest due to the discovery that nuclear reactions of unknown origin may occur when palladium is electrochemically loaded with a sufficiently high concentration of deuterium, as first reported in M. Fleischmann, S. Pons & M. Hawkins, "Electrochemically Induced Nuclear Fusion of Deuterium," J. Electroanal Chem., Vol. 261 (April 10, 1989), pp. 301-308. After this discovery, considerable controversy appeared in the scientific literature and popular press due to difficulty in demonstrating the effect, and due to the novel nature of the nuclear reaction causing the effect.

Various groups attempting electrolytic compression of deuterium into palladium have reported varying degrees of success, ranging from none, to in excess of about 70% (success being defined as the percentage of cells which produced tritium or neutrons in relation to the total number of cells operated) reported by the Bhabba Atomic Energy Research Center of Bombay, India, at the First Annual Conference on Cold Fusion in Salt Lake City, Utah, on March 28-31, 1990. (See page 80 of P.K. Iyengar and M. Srinivasan, "Overview of BARC Studies in Cold Fusion," Conference Proceedings of the First Annual Conference on Cold Fusion, Salt Lake City, Utah, March 28-31, 1991, pp. 62-81.)

Some aspects of the nuclear reaction mechanism are

presently understood with some certainty, although that understanding appears to contradict conventional theory of nuclear reactions. The reaction generates low levels of neutrons, much higher levels of tritium, and heat possibly in excess of that explained by the generation of neutrons or tritium. The reaction mechanism therefore appears to involve the fusion of deuterium to form neutrons and tritium, but the observed reaction rates are too high to be explained by any known kind of fusion reaction between deuterium at low temperature. More puzzling is the fact that the rate of tritium generation appears to be enhanced, relative to rate of neutron generation, by a factor on the order of about ten million. One possible explanation for such a reaction mechanism, for example, is Dr. Edward Teller's hypothesized catalytic neutron transfer and a three-body reaction promoted by standing de Broglie waves. Such a theory correctly presumes that a periodic structure can affect a nuclear reaction involving a nucleus in that structure, as is demonstrated by the Mossbauer effect (recoil-free emission and absorption of a gamma photon).

More recently a number of techniques have become known in the art for increasing the probability of success in demonstrating nuclear reactions when deuterium is electrolytically loaded into palladium. It is generally believed that a high loading ratio of deuterium to palladium is a pre-requisite for obtaining the nuclear reactions. It is suggested, for example, in T. Bressani, E. Del Giudice, G. Preparata, II Nuovo Cimento Note Breve, 101A, N5 845 (1989), that under certain conditions (at a deuterium-to-palladium loading ratio of 1:1) quantum-coherent phenomena may become important and D-D fusion may occur.

To demonstrate nuclear effects, it is known to electrolytically compress deuterium into a large number of palladium electrodes, measure the loading of each electrode

(for example by measuring the electrical resistance of the electrodes), and then select the electrodes having the highest loading ratios for placement in a limited number of calorimeter cells for measurement of heat production.

Due to the significance of the deuterium/palladium (D/Pd) ratio, considerable effort has been devoted to obtaining a reliable method for measuring the loading ratio. Typical techniques that have been employed are: 1) electrolytic discharge of the cathode resulting in the oxidation of the deuterium that had been absorbed by the palladium, 2) periodic weight measurements of the cathode and gravimetric determination of deuterium loading, 3) dilatometric experiments aimed at calculating loadings from length and width increases in the metal, 4) resistance measurements of the palladium cathodes during the deuterium loading process and 5) head space gas pressure or volume measurements monitoring increases of excess oxygen production.

Even though each of these techniques measure a variable that is proportional to deuterium loading, they all have drawbacks. The first technique is unreliable due to competing reactions taking place. Further, it does not give intermediate in-situ results because this process can only be done at the end of the experiment and only one value is obtained [See R. P. Adzic et al., Conference Proceedings of the First Annual Conference on Cold Fusion, Salt Lake City, Utah, March 28-31, 1990, pp. 261-271 at pp. 264-265.] The second technique does not allow one to determine loading curves in-situ. Because the sample must be taken out of the electrolytic cell, the weighing process introduces errors associated with spontaneous outgassing of the deuterium from the palladium [See D. J. Gillespie, G. N. Korun, A. C. Ehrlich, P. L. Mast, Fusion Technology 16, 526 (1989)]. The dilatometry method also has problems. Due to the fact that the deuterium will enter the palladium

so readily it has been shown that the palladium can fill to the point that it will crack and bulge the metal. This gives an overestimate of the amount of deuterium in the palladium. A few groups have applied resistance measurement techniques [See J. P. Burger, D. S. MacLachlan, R. Mailfert, B. Sonffache, Solid State Comm. 17, 277 (1975)]. Some of them have found that the curves are parabolic in shape which indicates a maximum resistivity. It appears that beyond this point the palladium deuterium cathode behaves as a semiconductor. Under these conditions, the resistivity measurements are not adequate for precise loading information.

A simple direct way to measure loading is by a volumetric measurement of the oxygen and deuterium produced during electrolysis. [See J. Divisek, L. Furst, J. Balej, J. Electroanal. Chem. 278, 99 (1990).] This technique has been used to measure loading as a function of time. The loading has been found to be generally in the range of 0.65 to 0.85 for the saturation or equilibrium atomic loading ratio, D/Pd. In most cases, prolonged electrolysis does not cause further increases in loading ratio and only in a few cases, loading ratios of approximately 1.0 may have been achieved but the reasons for this are obscure.

It is known to charge a hydrogen absorbing electrode in gradual fashion, for example by applying step-wise increases in the charging current, with a step-wise increase in current occurring after saturation is achieved during initial charging at a relatively low current level. As disclosed on page 23 of International Application No. PCT/US/90/01328, published on Sept. 20, 1990 as WO 90/10935, an example for charging is to charge a cathode at a relatively low current level of about 64 mA/cm^2 for about 5 diffusional relaxation times and then to progressively increase the current to levels of 128, 256, 512 mA/cm^2 or higher in order to facilitate heat generating events.

It is also believed that excess heat generation is sometimes initiated by introducing system perturbations. Scott et al., "Measurement of Excess Heat and Apparent Coincident Increases in the Neutron and Gamma-Ray Count Rates During The Electrolysis of Heavy Water," Fusion Technology, Vol. 18, Aug. 1990, pp. 103-114, for example, discloses on page 114 that a decrease in electrolyte temperature appeared to be most efficient for initiating excess power generation, and in two cases, increases in neutron count rate appeared to be related to system perturbations such as cathode current cycling or electrolyte temperature change. A closed-system test shown in FIG. 7 of Scott et al. included an interval of 1005 to 1170.5 hours in which the cathode current density was cycled between 100 and 400 mA/cm^2 for a cycle period of 66 minutes; this was followed by a second interval of cycling between 300 and 500 mA/cm^2 with a period of 5.7 minutes. But the effect of such cycling on deuterium loading was not established.

Pulsed cathode current was reported for a cell described on page 67 of P.K. Iyengar and M. Srinivasan, "Overview of BARC Studies in Cold Fusion," Conference Proceedings of the First Annual Conference on Cold Fusion, Salt Lake City, Utah, March 28-31, 1991, pp. 62-81.) At first a current of 1 ampere was used for the electrolysis. After about 30 hours of operation, current pulsing between 1 and 2 ampere at one second intervals was adopted. After a charge of 17.5 ampere-hours had been passed, the first neutron emission was detected. As shown in Fig. 6 (of Iyengar et al.), three distinct neutron bursts of 14 to 20 minutes duration each were produced amounting to an integrated yield of 3×10^6 neutrons. Subsequent analysis of a sample of the electrolyte indicated that a total of 3.85 μCi or 7.3×10^{13} atoms of tritium had been generated in the experiment.

Cathode current reverses have been reported during electrolytic tritium production. See Fig. 2 on page 682 of E. Storms and C. Talcott, "Electrolytic Tritium Production," Fusion Technology, Vol. 17, July 1990, pp. 680-695.

SUMMARY OF THE INVENTION

Briefly, in accordance with a basic aspect of the invention, isotopic hydrogen such as deuterium is electrolytically loaded into a hydrogen absorbing electrode by alternately charging and discharging the electrode in a plurality of cycles, each cycle including charging of the electrode with isotopic hydrogen approximately to a saturation level and then discharging of the electrode to a predetermined retention level. Preferably the electrode is charged approximately to a saturation level by charging for a predetermined duration of time, and the electrode is discharged to a predetermined retention level by discharging until a predetermined cell voltage threshold is reached at a predetermined discharge current.

In an aqueous electrolyte, for example, the predetermined cell voltage threshold is a positive voltage on the electrode such as 0.8 volts that is just below the voltage (about 1.2 volts) at which oxygen evolution at the electrode could thermodynamically occur. Moreover, when an aqueous electrolyte is used, preferably the electrolytic cell includes a microporous separator preventing recombination on the palladium cathode of isotopic hydrogen being discharged from the electrode with oxygen having been generated during the charging of the electrode.

Preferably charging for each cycle is performed up to a maximum rate that is decreased for subsequent cycles following an initial cycle. Preferably the electrode is discharged abruptly during each cycle, for example by ramping-down or stepping-down a cell current set-point

while limiting the magnitude of the discharge voltage to the predetermined cell voltage threshold at which discharging is terminated.

Preferably palladium or palladium alloy electrodes are pre-treated by palladizing to deposit a thin surface layer of palladium black, and then the electrodes are pre-loaded with isotopic hydrogen gas in a gas-filled vessel.

In a specific example, a 2 mm diameter Pd wire purchased from Hoover & Strong, Inc. (99.99% purity) is palladized by electrodeposition of a thin coating of Pd black, then pre-loaded in deuterium gas at approximately atmospheric pressure for about 12 hours, then immediately transferred to an electrochemical cell having a 0.5 M D_2SO_4 in D_2O electrolyte, initially charged electrolytically at current density of 10-50 milliamps/cm^2 for 1,000 to 2,000 minutes, then discharged at current densities sequentially of 30, 10, and 5 milliamps/cm^2 while limiting the cell voltage to below 1 volt to avoid oxygen evolution on the palladium electrode, immediately followed by reloading the electrode with deuterium, employing a current density of 10 or 20 milliamps/cm^2 for at least 1,000 minutes, and repeating discharging and charging under these conditions for a total of 4-5 times. This procedure leads to a stepwise increase in the D/Pd loading ratio, ultimately obtaining loading ratios in the vicinity of 1. This procedure has been successful in 4 out of 4 experiments for consistent reproduction of the high loading ratio and consistent reproduction of tritium generation. No tritium generation was observed in four H_2SO_4 control cells operated simultaneously. Evidence for neutron generation was also observed from all four D_2SO_4 cells. A single anomalous temperature excursion was observed in one of the four cells.

BRIEF DESCRIPTION OF THE DRAWINGS

Other objects and advantages of the invention will

become apparent upon reading the following detailed description and upon reference to the drawings in which:

FIG. 1 is a schematic diagram in cross-section of a test cell used for loading ratio and tritium generation experiments;

FIGS. 2A and 2B are graphs of the deuterium to palladium loading ratio, and the hydrogen to palladium ratio, respectively, as a function of time obtained in a pair of cells wired in series to have a similar cycling of cell current in accordance with the present invention during one experiment;

FIGS. 3A and 3B show results of an experiment similar to that reported in FIGS. 2A and 2B, but with a decrease in current density during a latter portion of a first cycling of the cell current;

FIGS. 4A and 4B show results of a loading experiment using a palladizing pre-treatment of the palladium electrode to obtain a small increase in the loading ratios;

FIGS. 5A and 5B show results of a loading experiment using gas-phase pre-loading of palladized palladium electrodes with deuterium or hydrogen, respectively, to obtain an additional small increase in the loading ratios;

FIGS. 6A and 6B show results of a loading experiment using gas-phase pre-loading of palladium electrodes, but without using a palladizing pre-treatment, and using a single cycling of the loading current followed by pulsing of the loading current;

FIGS. 7A and 7B show graphs of the deuterium to palladium loading ratio, and the temperature of the palladium and platinum electrodes, in a deuterium cell during a loading experiment with a palladized palladium electrode;

FIGS. 8A and 8B show the results in a hydrogen cell during the experiment also reported in FIGS. 7A and 7B;

FIGS. 9A to 9E show graphs of data from a set of

tritium generation experiments; in particular, FIG. 9A shows a graph of the deuterium to palladium loading ratio as a function of time for a second one of the tritium generation experiments, FIG. 9B shows a graph of the electrode temperatures as a function of time in a deuterium cell for the second one of the tritium generation experiments, FIG. 9C shows a graph of the hydrogen to palladium loading ratio as a function of time for the second one of the tritium generation experiments, FIG. 9D shows a graph of the deuterium to palladium loading ratio as a function of time for a third one of the tritium generation experiments, and FIG. 9E shows a graph of the hydrogen to palladium loading ratio as a function of time for the third one of the tritium generation experiments;

FIG. 10 shows the tritium distribution observed in four palladium cathodes from deuterium cells after four respective tritium generation experiments;

FIGS. 11A and 11B show neutron count data for the deuterium cells in the first and third tritium generation experiments, respectively.

FIGS. 12A and 12B show the electrical power input, and the temperatures observed for the palladium and platinum electrodes, respectively, during a latter portion of the second tritium generation experiment;

FIGS. 13A and 13B show expected cell potential and programmed cell current in a system wherein a cell is controlled in accordance with the invention by operating a digital computer;

FIG. 14 is a block diagram of a system including a battery of cells and a digital computer for cycling the current in each of the cells in accordance with the invention;

FIG. 15 is a schematic diagram of a thermistor bridge and amplifier circuit used in the block diagram of FIG. 14;

FIG. 16 is a schematic diagram of a cell power supply used in the block diagram of FIG. 14;

FIG. 17 is a flowchart of a program executed by the computer in the system of FIG. 14 for cycling the current in each of the cells in accordance with the invention;

FIG. 18 is a flowchart of a sample timer interrupt routine that the digital computer of FIG. 14 executes at periodic sample times to collect cell data and to change the cell currents;

FIG. 19 is a flowchart of a routine executed once for each cell at each sample time, in order to determine whether the current for each cell should be changed at each sample time, and if so, to change the cell current and to compute the next time that the current for the cell should be changed; and

FIG. 20 is a flowchart of a routine executed to repeat cycling of cell current in accordance with the invention, beginning with a first discharge cycle, in an attempt to restore a high loading ratio in the cell.

While the invention is susceptible to various modifications and alternative forms, specific embodiments thereof have been shown by way of example in the drawings and will be described in detail herein. It should be understood, however, that it is not intended to limit the invention to the particular forms disclosed, but on the contrary, the intention is to cover all modifications, equivalents, and alternatives falling within the spirit and scope of the invention as defined by the appended claims.

DETAILED DESCRIPTION OF THE PREFERRED EMBODIMENTS

I. Working Examples

A. Loading Experiments.

A volumetric technique was used for continuous measurement of respective deuterium and hydrogen uptake during loading of palladium cathodes while imposing non-steady state diffusion conditions upon the cathodes. We

were interested in elucidating the conditions necessary to reach a loading ratio of 1:1 (D or H:Pd) and the time required to achieve such ratios. Two parallel experiments were conducted, one with deuterium and the other with hydrogen, in order to compare the loading ratios obtained under otherwise identical conditions.

1. Loading Measurement Cell System.

The hydrogen or deuterium uptake was determined by a volumetric measurement of the difference between the D_2 or H_2 and the O_2 liberated under electrolysis. The experimental electrochemical cell 20, which was fabricated from laboratory grade glassware, is shown in FIG. 1. The cell 20 eliminated contact between hydrogen or deuterium and oxygen gas by using a fritted glass cell divider 21 between the cathode 22 and the anode 23 of the cell. The fritted glass cell divider 21 was in the form of a fritted glass cylindrical tube 2.5 cm diameter x 3.0 cm long in coaxial relationship with the cathode 22 and the anode 23 and separating a cathodic compartment 24 from an anodic compartment 25. The fritted glass tube 21 had holes of 200 microns porosity through which electric current was passed while preventing recombination of the deuterium or hydrogen and oxygen discharged from the electrodes.

The cathode 22 was a 1.0 mm diameter by 3.0 cm long cylindrical wire placed at the center of the cell 20. The anode 23 was a cylindrical piece of 0.1 mm thick Pt foil surrounding the fritted glass tube to provide uniform current distribution during electrolysis. The cathodic compartment 24 and anodic compartment 25 were separated on the bottom part of the cell 20 with a "TEFLON" (polytetrafluoroethylene) holder 26, which had channels 27 for flow of electrolyte 28 to equalize the electrolyte levels in the cathodic compartment 24 and anodic compartment 25. Electrical and thermistor lead wires 29 extended through the top of the cathodic compartment 24 and

a stopper 30 and connected to a power supply and computing system (not shown).

To determine possible temperature excursions produced by nuclear reactions, two calibrated thermistors 31, 32 were used. One of these 31 was employed to measure the cathode temperature. It was enclosed in a glass capillary tube 33 and bonded to the cathode with thermally conductive epoxy. For still better heat conduction, the thermistor 31 was embedded in thermal joint compound inside of the glass capillary tube 33. The second thermistor 32 was employed to measure the temperature in the anode compartment 25. It was positioned as close as possible to the Pt foil of the anode 23.

Both the cathodic and anodic compartments 24, 25 had two fittings 35, 36 and 37, 38 each for gas inlet and outlet. The cathodic and anodic compartments 24, 25 were connected by an exterior loop 39 through valves 40, 41 so that the gases could recombine on a platinum catalyst 42 placed above the anode electrolyte. The electrolyte volume in the cell was approximately 38 cm^3, whereas the total gas volume was approximately 300 cm^3.

A water-filled manometer 43, comprised of two burets 44, 45 which were connected at their lower ends with flexible tubing 46, was connected to the port 38 of the cell 20 through a valve 47. The manometer 43 was used to measure changes in the gas volume above the electrolyte 28. A first buret 44 was initially filled with water 48. By adjusting the relative height of the second buret 45, the pressure in the cell 20 was maintained at atmospheric pressure. All joints were of ground glass, greased with silicone to ensure a vacuum-tight system.

The system was kept at constant pressure, so that the resulting decrease in the gas volume of the cell 20 was a direct measure of the quantity of deuterium or hydrogen absorbed by the palladium cathode 22. Corrections were

made for atmospheric pressure and temperature. The system was regularly tested for leaks by moving the second adjustable buret 45 and pressurizing the cell.

All experiments were performed with two identical cells, submerged totally in two separate water baths (not shown), held as close to room temperature as possible (27°C ± 0.1°C).

2. Measurements.

During the loading experiments, the following data were collected and stored:

1) Applied current for electrolysis during charging and discharging experiments, using a Keithley 228A current source or an EG&G Potentiostat/Galvanostat for the power supply.

2) Potential of each cell during the cycling experiments measured with a Keithley 179 Multimeter and collected data by HR 2300 Hybrid Recorder.

3) Measurements of volume oxygen change during cycling experiments (±0.1 ml).

4) Measurements of air temperature (±0.1°C) and pressure (±0.1 mm Hg).

5) Measurements of the respective temperatures of the cathode and anode with thermistors (±0.05°C), and data collected by a computing system (Macintosh IIx).

3. Materials and Reagents.

The majority of the experiments were carried out using a 0.5 M H_2SO_4/H_2O electrolyte for the hydrogen cell (hereinafter the "H" cell) and 0.5 M D_2SO_4/D_2O electrolyte for the deuterium cell (hereinafter the "D" cell). These acidic electrolytes were more suitable for a fritted glass cell than alkaline solutions. The heavy water (99.9%) was purchased from Cambridge Isotopes Laboratories Ltd. and in all but one case had a tritium content of 27 ± 1 dpm/ml. The D_2SO_4 solution was made by diluting concentrated D_2SO_4 (98%; Aldrich Chem. Co. Inc.) in D_2O, and the H_2SO_4 solution

was made by diluting concentrated H_2SO_4 (96%; Baker Analyzed Reagent) in H_20. Deuterium gas (99.99% purity UN1954 from Cryogenic Rare Gas Comp.) and hydrogen gas (96% from US Welding Comp.) were used. Palladium was obtained from Aesar (Johnson Matthey; 1 mm diameter wire; 99.995% purity). The palladium as received from the manufacturer was wiped clean with a clean paper tissue wetted with deionized water.

In several experiments, the surface of a palladium cathode 22 was activated by electrodepositing palladium black onto the surface of a palladium rod. For the palladium cathode used in "D" cell, the palladizing solution was 0.05 M $PdCl_2$ in 0.1 M DCl and for Pd-cathode used in "H" cell palladizing solution was 0.05 M $PdCl_2$ in 0.1 M HCl. Palladizing conditions were 20 mA/cm^2 current density for 60 seconds in both experiments.

In a few experiments, the palladium cathodes were preloaded with D_2 or H_2 in a gas-phase system.

Platinum foil (0.1 mm thick: 99.98%) obtained from Johnson Matthey Electron., was used to fabricate the cylindrical anode 23. The anode was provided with a platinum black layer, by electrodepositing platinum black from a $PtCl_2$ solution.

For the recombination catalyst 42, a piece of Fuel Cell Grade Pt Catalyst on Ag plated Ni screen (ESN) electrode (E-TEK Inc.) was used.

4. Results.

In a typical loading (charging) experiment, the electrolytic cell was initially evacuated and then refilled with D_2 or H_2 gas of ambient pressure. The palladium electrode 22 was made cathodic and a constant charging current of 50, 20 or 10 mA/cm^2 was passed through the cell. During this loading process, a fraction of the deuterium (or hydrogen) produced at the cathode 22 was absorbed by the palladium, and oxygen was liberated at the anode 23.

This oxygen was catalytically recombined with deuterium (or hydrogen) gas in the oxygen compartment of the cell at the catalyst 42 to form liquid water. Since the system was kept at constant atmospheric pressure by adjusting the water level in the burets 44, 45, the resulting decrease in the gas volume of the cell 20 was a direct measure of the quantity of deuterium (or hydrogen) absorbed by the palladium.

In an unloading (discharging) experiment, the palladium electrode 22 was made anodic and sequential constant discharging currents of 30, 10 and 5 mA/cm^2 through the cell. The voltage of the cell was monitored and the discharge current was decreased to the next lower value when the cell voltage reached 0.8 V. Under these conditions, the main reaction occurring on the palladium electrode 22 was the oxidation of deuterium atoms, diffusing out of the palladium, to D+ ions (see equation (1) below). Depending on the surface activity of the palladium electrode, recombination of D atoms to form D_2 gas may also take place to a minor extent (see equation (2) below). Due to the fact that the cell potential is kept below 0.8 V, oxygen evolution did not take place. Deuterium gas was generated on the platinum electrode 23, and therefore the resulting increase in the gas volume of the cell was a direct measure of the quantity of deuterium (or hydrogen) diffusing from the palladium electrode. The reactions on the palladium electrode during discharging (anodic unloading) were:

$$2D_{(Pd)} \rightarrow 2D^+ + 2e^- \qquad (1)$$

and on the platinum electrode was:

$$2D^+ + 2e \rightarrow D_2 \qquad (2)$$

The overall reaction was:

$$2D_{(Pd)} \rightarrow D_2 \qquad (3)$$

and depended on the diffusion of deuterium (or hydrogen) from the palladium electrode. In this case, we eliminated

the possibilities of spontaneous recombination of deuterium (or hydrogen) and oxygen on the immersed palladium electrode surface because no oxygen is generated in the cell during discharging, and we minimized the possible factors of error in measuring the changing of the gas volume in the system. The total error in estimating the loading ratio of palladium with deuterium (or hydrogen) absorbed into the palladium was believed to be less than 5%.

Data from a typical loading experiment are shown in FIG. 2A for the "D" cell and in FIG. 2B for the "H" cell. After 20 hrs loading at 50 mA/cm^2 current density in the acidic electrolyte, the loading level achieved was similar to typical results obtained in LiOD or LiOH electrolyte (0.58 for D:Pd ratio and 0.64 for H:Pd ratio). These ratios, however, were increased by cycling of the electrolytic current, and reached values of about 1.0 for both cathodes (deuterium and hydrogen) after a total of 150 hours of operation. After each discharging cycle, each of which lasted approximately three hours and consisted of discharge current sequences of 30, 10 and 5 mA/cm^2 current density and voltages below 0.80 volts to prevent oxygen evolution, all charging cycles were carried out at 10 mA/cm^2 current density for periods of time from 15 to 70 hrs. The high loading ratio (D/Pd or H/Pd about 1:1) was achieved after the 5th cycle of charging and discharging the cell, as shown in FIGS. 2A and 2B.

FIGS. 3A and 3B show the effect of decreasing the current density during the first cycle of loading. Reducing the current density from 50 mA/cm^2 (after about 2 hrs charging) to 10 mA/cm^2 only slightly improved the loading ratio (D/Pd = 0.60; H/Pd = 0.74).

FIGS. 4A and 4B show a similar experiment using palladized cathodes. This experiment shows that a small increase in the loading ratio was observed when palladizing

surface pre-treatment of palladium was used. The loading rate was considerably faster than in the experiment using a non-palladized palladium cathode.

FIGS. 5A and 5B show another experiment in which the palladium cathodes were palladized and pre-loaded with deuterium or hydrogen in the gas phase. The degree of pre-loading was calculated from pressure drop measurements and verified by mass differences.

FIGS. 6A and 6B show a loading experiment for pre-loaded cathodes without palladizing. FIGS. 5A, 5B, 6A and 6B together show that a small increase in the loading level was observed for cathodes pre-treated by palladizing the surface compared to as-received palladium.

FIGS. 6A and 6B also show long term electrolysis of Pd cathodes (pre-loaded with D_2 or H_2) after a first cycling experiment. As a result of the first cycling experiment, a loading ratio plateau 61 of about 0.79 for D/Pd and a loading ratio plateau 62 of about 0.94 for H/Pd was overcome by a discharge cycle at about 1500 minutes. The palladium electrodes were then loaded at 10 mA/cm^2 current density for ~100 hrs and then for ~30 hrs palladium cathodes were loaded using variable current density in which the current density was alternately switched at 30 minute intervals between 10 and 20 mA/cm^2. FIGS. 6A and 6B each show respective final plateaus 63, 64 of maximum loading level (D/Pd = 0.86 and H/Pd = 0.98) which were not changed despite the variable current density over a long period of time.

Comparisons of the relative loading rates between hydrogen and deuterium in palladium in all experiments show that the loading rate in the deuterated solution is faster than for the light-water electrolyte. This is understandable because deuterium has a higher diffusion coefficient than hydrogen in palladium. Also the maximum loading levels for palladium obtained in "D" and "H" cells

show a slightly higher level of loading for H/Pd than for D/Pd in all of our experiments.

Two typical electrolysis experiments with 1-mm diameter palladium wires (palladized before being used) are shown in FIGS. 7A and 7B for the "D" cell, and 8A and 8B for the corresponding "H" cell. The D/Pd and H/Pd loading ratios are shown in FIGS. 7A and 8A, respectively. We observed small temperature differences of the cathodes corresponding to the charging and discharging cycles, but we did not observe any significant rising of temperature of cathodes during the loading cycles. The temperatures of the electrodes were measured with a sensitivity of 0.05°C and response time of a few seconds.

The experiments of FIGS. 8A to 9B were concluded after discharging cycles, and the cathodes were taken out of the cells, washed and weighed. The cathodes were degassed in a nitrogen atmosphere at 370°C over 24 hours. From the mass differences of cathodes before and after the loading experiment, we found the loading ratio for D/Pd = 0.68 and for H/Pd = 0.75, which compares favorably with loading ratios from volumetric measurements (D/Pd = 0.75 and H/Pd = 0.83). The differences were less than 10%.

5. Conclusions.

The volumetric method was adopted for continuous measurement of the absorption of deuterium (or hydrogen) by palladium during the electrolysis of heavy-water (or light-water) in acidic electrolytes. The electrolytic cell was designed to eliminate contact between oxygen and palladium and, hence, spontaneous recombination between D_2 (or H_2) and O_2 at the palladium electrode. The discharging cycles were run at controlled current with a maximum cell voltage below 0.80 volts. The accuracy of the volumetric techniques for loading measurements was confirmed by mass measurements on a 1 mm palladium wire. The accuracy was about 5%.

Loading ratios of approximately 1.0 have been

achieved when suitable cycling conditions were used for loading and unloading. The first loading cycle was carried out at 10 to 50 mA/cm^2 current density for 20 to 50 hrs respectively, but each subsequent loading cycle was carried out at lower current density (~10 mA/cm^2). It appears that carrying out each subsequent loading cycle at lower current density should be done to achieve a maximum loading ratio of 1.0. Each cycle increased the loading ratio by a factor of about 0.05 to 0.1, and a loading ratio of about 1.0 was achieved after the 5th cycle. The normal charging time between discharge cycles should be at least 15 hrs. However, prolonged electrolysis at constant current does not cause further significant increases in loading ratio.

The surface pre-treatment by palladizing the surface of the cathodes does not appear to increase the final loading ratios significantly but increases the rate of loading and unloading. Using cathodes pre-loaded in the gas phase also does not appear to increase the final loading level. However, the gas pre-loading of cathodes decreases the number of cycles needed to achieve the high loading ratios. In addition, palladizing prior to gas pre-loading decrease the time required for gas pre-loading from about 12 hours to about 3 hours.

The highest atomic loading ratios obtained in the electrolysis of heavy and light-water acidic electrolytes were D/Pd = 1.01 ($\pm$0.05) and H/Pd = 1.10 ($\pm$0.05).

B. Tritium Generation Experiments

In this series of experiments, tritium generation was consistently reproduced in four out of four electrolytic cells having palladium cathodes of 2 mm diameter. Deuterium loading ratios near or slightly higher than unity were obtained in these palladium cathodes by the current cycling procedure previously used in the loading experiments described above. The hermetically sealed cell design of FIG. 1 was used. The tritium content of the

electrolyte, the Pd and the gas above the electrolyte is determined prior to and after an experiment. Therefore, any increase in tritium content could have only originated from nuclear reactions occurring during the experiment. A light water control cell was always run in electrical series to every D_2O cell under essentially identical conditions. This procedure always permitted direct comparison of any tritium, neutron or excess heat generation in the D_2O cell and the H_2O control cell.

In the tritium generation experiments, 2 mm diameter palladium wire cathodes were used (Hoover & Strong, Inc., 99.9% purity). The cathodes, as received from the manufacturer, were wiped clean with a clean paper tissue wetted with deionized water, palladized as described above, and pre-loaded overnight with isotopic hydrogen gas at approximately atmospheric pressure. In three of the four experiments, the palladium cathodes were electrolytically charged in an initial cycle up to a maximum current density of 50 mA/cm^2; in the other experiment, the palladium cathode was electrolytically charged in an initial cycle up to a maximum current density of 20 mA/cm^2.

In one of the four experiment, Li_2SO_4 (solid 99.99% from Aldrich Chem. Corp. Inc.) was added to the acids. Deuterium gas was purchased from Air Products & Chemicals Inc. and Alphagaz-Liquid Air Corp. Both suppliers use heavy water electrolysis to produce D_2 gas, and both purchase the heavy water from the same source, Ontario Hydro (Canada). It can be assumed that any tritium contamination in the D_2 gas originates from this heavy water and therefore should be similar for both gas suppliers. The level of tritium contamination in the D_2 gas is given as less than 5 nCi/liter gas, which is the detection limit of the suppliers' chemical analysis. Otherwise, the materials and reagents for the tritium generation experiments were the same as described above for the

loading experiments.

Since an accurate value of the tritium contamination level was not supplied for the deuterium gas, a tritium analysis procedure for D_2 gas was developed. The recombination reaction of D_2 with O_2 gas on a catalyst surface (not shown) was used to obtain aliquots of heavy water for analysis. A gas-tight vessel was connected to a gas buret (not shown) to measure the volume of D_2 gas recombined. An evacuated vessel (not shown) containing a 12 cm^2 piece of catalyst (not shown) was filled with the D_2 gas. Oxygen was injected with a syringe (not shown) through a septum (not shown) and the deuterium displacement was measured. The recombined heavy water was rinsed out with distilled water and analyzed for tritium in a Beckman LS5000 TD Liquid Scintillation Counter. The tritium content was found to be 0.13 to 0.14 nCi/liter of D_2. This value was in good agreement with values obtained by Dr. Claytor at Los Alamos National Laboratory on a D_2 tank provided to him.

1. Instrumental Setup.

All experiments were performed with an identical light water control cell run in electrical series to the heavy water cell. The two cells were contained in two separate water baths of type EX-510D from NESLAB Inst. Inc., which controlled the temperature to $\pm$ 0.1°C. The following data were measured or collected with the following instrumentation:

1) Applied current for electrolysis: Keithley 228A Current Source or EG&G Potentiostat/Galvanostat.

2) Potential: Keithley 179 Multimeters and Yokogawa HR 230 Hybrid Recorder.

3) Potential of cathode vs. reference electrode (where applicable) Keithley 179 Multimeters and HR 2300 Hybrid Recorder.

4) Temperatures of the cathode and anode:

Thermistors (± 0.02°C) of type SP60BT 103M1 from Thermometrics, Inc.; stored in a MacIntosh 11X computer with an Omegabench software program from Omega Engineering, Inc.

5) Gas volume measurements were made with a water manometer to an accuracy of ± 0.1 ml; air temperature and air pressure were monitored with an accuracy of ±0.1°C and ±0.1 mm Hg, respectively.

6) Neutron detection was performed with ^{3}He tubes. Two tubes each were used to monitor the light and heavy water cells, respectively. They were installed and positioned at a distance of 7 cm from the electrolysis cells in the water baths. To prevent cross talk between the ^{3}He tubes for the light and heavy water cells, they were spaced 1 m apart and separated by a layer of borate-impregnated paraffin bricks. Neutron data were recorded with an IBM computer system.

2. Experimental Procedure.

Before each experiment, the tritium contents of the electrolyte, representative pieces of the Pd, and the D_2 fill gas were determined. The Beckman LS5000 TD was employed for tritium counting. The electrolytic cells were evacuated and then refilled with D_2 and H_2 gas of ambient pressure. This assured proper and immediate functioning of the internal gas recombination catalyst. When starting the electrolysis, which was always conducted with the same current flowing through both the D_2 and H_2 cells, essentially no D_2 or H_2 gas was generated on the Pd. The O_2 gas, generated on the Pt anodes, recombined with the pre-filled D_2 or H_2 to form water. The amount of D_2 or H_2, consumed by reaction with the O_2, was precisely equivalent to the number of D or H atoms absorbed by the Pd. Hence, the decrease in the gas volumes in the cells was a precise measure for the D/Pd and H/Pd loading ratio, respectively. The gas volume stopped changing when full loading was

attained.

After completing an experiment, which generally lasted for about one week, the electrolyte, Pd electrode and gas were analyzed again for tritium and compared to the tritium amounts present before the experiment.

Since we analyzed for all the tritium in the cell before and after an experiment and since the cell was sealed during the experiment, any increase in tritium level could only have resulted from tritium generation in the experiment itself. Considerations regarding deuterium-tritium partitioning between gas, electrolyte and Pd were therefore eliminated.

3. Results and Discussion

Typical results of our loading ratio measurements as a function of time are presented in FIGS. 9A to 9E. The second electrolytic deuterium loading experiment (Experiment #2 in TABLE I below), for example, was performed for 12 days. The electrodes were initially charged electrolytically at current densities up to 20 or 50 milliamps/cm^2 for 1,000 to 2,000 minutes, then discharged at current densities sequentially of 30, 10, and 5 milliamps/cm^2 while limiting the cell voltage to below 1 volt to avoid oxygen evolution on the electrodes, immediately reloaded with hydrogen or deuterium at a current density of 10 or 20 milliamps/cm^2 for at least 1,000 minutes, and repeatedly discharged and charged under these conditions for a total of 4 to 5 times. At the start of applying an electrolytic current, the loading ratio already had a finite value, which for the deuterium cell was 0.68 (FIG. 9A) and for the hydrogen cell 0.75 (FIG. 9C). The loading curves in FIGS. 9A and 9C for this second experiment show a rise in the loading ratio to values of about 0.95. The loading ratio in the deuterium cell appears to continue increasing (FIG. 9A) whereas the loading ratio in the hydrogen cell appears to be saturating

Table 1

Tritium Analysis of Electrolyte, Pd and Gas

Exper. #		1		2		3		4	
Time at LR > 0.85 [h]		163.8		169.7		144.4		161.3	
Electrolyte		D_2SO_4 +Li_2SO_4	H_2SO_4 +Li_2SO_4	D_2SO_4	H_2SO_4	D_2SO_4	H_2SO_4	D_2SO_4	H_2SO_4
Loading Ratio Atom Fraction		0.99	1.030	0.96	0.95	1.02	1.07	1.15	1.01
#T atoms Electrol.	Before	3.8×10^{9}	ND	2.9×10^{9}	ND	1.0×10^{11}	ND	2.4×10^{9}	ND
	After	1.9×10^{11}	ND	8.0×10^{10}	ND	1.4×10^{11}	ND	8.7×10^{10}	ND
#T atoms in Pd	Before	ND	ND	ND	ND	ND	ND	ND	ND
	After	1.7×10^{10}	ND	1.6×10^{10}	ND	2.1×10^{10}	ND	ND	ND
#T atoms Gas	Before	1.8×10^{8}	NM	1.8×10^{8}	NM	1.8×10^{8}	NM	1.8×10^{8}	NM
	After	1.8×10^{8}	NM	8.3×10^{8}	NM	6.2×10^{9}	NM	NM	NM
#T atoms Total	Before	4.0×10^{9}	ND	3.1×10^{9}	ND	1.0×10^{11}	ND	2.6×10^{9}	ND
	After	2.1×10^{11}	ND	9.7×10^{10}	ND	1.7×10^{11}	ND	1.3×10^{11}	ND
T Generated [# atoms]		2.1×10^{11}	ND	9.4×10^{10}	ND	7.0×10^{10}	ND	1.3×10^{11}	ND
Enhancement Factor		52.5	ND	31.2	ND	1.7	ND	50.0	ND
T Generated [# atoms/cm^2]		1.1×10^{11}	ND	4.5×10^{10}	ND	4.3×10^{10}	ND	6.5×10^{10}	ND
T Generate Rate [# atoms/cm^2/S]		2.0×10^{5}	ND	7.4×10^{4}	ND	8.3×10^{4}	ND	5.8×10^{4}	ND

• = Batch of D_2O with high T content

ND = Not Detected

NM = Not Measured

LR = D/Pd or H/Pd Loading Ratio

(FIG. 9C). Actually, the tendency to saturate is observed in most cases.

(a) Tritium Generation.

The electrolyte, palladium, and gas above the electrolyte in each D_2 cell were analyzed for their tritium contents before and after each experiment. In the H_2 cells, only electrolyte and Pd were analyzed. Table 1 below summarizes the tritium analysis results for all four experiments. We have found in other experiments that tritium is generated predominantly at loading ratios in excess of 0.85. Table 1 lists in the first horizontal column the times at which this loading ratio is attained in the four experiments. Table 1 also gives the maximum loading ratios that were achieved in the four experiments, comprising four D_2 cells and four H_2 cells. The loading ratios lie between 0.95 and 1.15, with an experimental uncertainty of $\pm$ 0.05. Tritium was not detected in any of the four H_2 control cells. On the other hand, significant tritium enhancements were found in all four D_2 cells, in particular, in the electrolyte and in the palladium. The total amount of tritium contained in the gas phase was relatively small. But an increase in this small tritium level in the gas phase was observed in two cases. The total amount of tritium generated in these four sealed cells is surprisingly uniform, from a low value of 7×10^{10} to a high value of 2.1×10^{11} T atoms. As the palladium cathode area in all four cells was approximately 2 cm^2, the number of T atoms generated in the four cells was also in a relatively tight band, from 4.3×10^{10} to 1.1×10^{11} T atoms/cm^2. These values are in good agreement with the values obtained by several research groups at the Bhabha Atomic Research Center in Bombay, India. Their values run from a low of 5×10^{9} to a high value of 1.7×10^{14} T atoms/cm^2. Predominantly, however, their values are in the range from 10^{10} to 10^{11} T atoms/cm^2, and their experiments

were run for comparable lengths of time as our experiments.

The average tritium generation rate in our experiments varies from 5.8×10^4 to 2.0×10^5 T atoms/cm^2/sec. In calculating this rate, the time prior to attaining loading ratio of 0.85 was not counted, as we have evidence for little or no tritium generation at loading ratios smaller than 0.85. We have calculated a tritium "enhancement factor" which expresses the ratio of the total tritium present in the cell after the experiment to the total tritium present before the experiment. Three of the four cells show enhancement factors from 31 to 52. The fourth cell has an enhancement factor of only 1.7, owing to the fact that in this cell a new batch of heavy water was inadvertently used with a tritium contamination level 30-40 times larger than the normal tritium content of the heavy water we have used. The analysis results of the heavy water were obtained only after the electrochemical experiments had been started.

Strikingly, none of the four H_2 control cells showed any detectable tritium in the electrolyte, or the palladium cathodes after the experiment.

Since we employed hermetically sealed cells in these experiments, and since we analyzed for total tritium content before and after the test, we can only come to the conclusion that the tritium that we find at the end of the experiments has been generated in or on the palladium cathodes during heavy water electrolysis.

The tritium analysis of the palladium cathodes was carried out by analyzing several small pieces cut from the entire electrode. The four samples for analysis were cut one each from the two ends and two from near the center of the cathode. The only exception was the palladium cathode used in experiment three in which the entire electrode was cut into four pieces.

Shown in FIG. 10 are the tritium distributions in

the four Pd cathodes in T atoms/g Pd. Significantly, in the three experiments where the ends of the palladium wires were analyzed separately from the center sections, comparatively much less tritium was found in the ends of the wires as compared to the center. (In FIG. 10, "ND" is an abbreviation for "none detected" and means that any tritium present was below the detection of about 5×10^8 tritium atoms/g.) The eight pieces near the center of the four electrodes showed a surprisingly tight band of values, namely from 1.2×10^{10} to 8.9×10^{10} T atoms/g Pd. It appears that the ends of the Pd wires either did not charge as efficiently as the center regions or that tritium escaped from the ends more readily.

The detection limit of our analytical procedure was 5×10^8 T atoms/g Pd. Therefore, the tritium levels that we found in the Pd after electrolysis are up to 178 times larger than the maximum possible contamination level before electrolysis. In previous analysis of over 100 as-manufactured palladium samples from the same supplier as the present palladium cathodes, we have found no evidence for tritium contamination within the detection levels of our procedure. Therefore, we conclude that the tritium found in the palladium cathodes has been generated by nuclear phenomena occurring in the deuterium-loaded palladium.

Two experimental observations made in this study indicate that the tritium was generated in the interior of the palladium rather than at its surface: 1) Tritium generation appears to be related to the D/Pd loading ratio; this would not be the case if tritium generation were a surface phenomenon. 2) Tritium is evidently emerging from the palladium during our analytical procedure which involves dissolution of the palladium of aqua regia; if the tritium were adsorbed on the surface of the palladium, it would be very unlikely that it would survive several

minutes of exposure to air during the cutting procedure and the transfer into the analytical system.

(b) Neutron Generation.

Neutron measurements on the electrolytic cells were carried out during the entire period of experimentation, that is for two months. Two ^3He counters each were positioned next to the D_2 and H_2 cell, respectively. The detectors were capable of detecting neutron emissions in a time gate as small as 8 μsec. Reported here, however, are only events involving three or more neutrons, counted in less than 1 millisecond. We have consistently found significantly larger numbers of triple events in the D_2 cells than in the H_2 cells. The results of the neutron counting are presented in Table 2. It is seen that the number of triples monitored on the four D_2 cells is consistently between a factor of 2.0 and 2.6 higher than in the H_2 cells. In the entire two month period of observation, the total number of triples is 51 for the four D_2 cells and 22 for the four H_2 cells.

Furthermore, we find the occurrence of two quadruple neutron events in the D_2 cells and one quadruple in the H_2 cells. FIG. 11A shows the quadruple neutron event monitored in experiment #1, and FIG. 11B shows the quadruple neutron event monitored in experiment #3. It is seen that the first event consists of 4 neutrons counted in 320 μsec whereas in experiment #3 the 4 neutrons are counted in 120 μsec. While the number of neutron events involving triplets and quadruplets detected in our experiments is quite small, we regard their consistently more frequent occurrence in the D_2 cells as compared to the H_2 controls as significant. Conducting the neutron detection in an underground laboratory would significantly reduce the background and lead to firmer conclusions.

Table 2

Triple and Quadruple Neutron Counts in D_2SO_4 (D) and H_2SO_4 (H) Cells

Experiment #	1		2		3		4	
Electrolyte	D	H	D	H	D	H	D	H
# Triples	13	5	14	7	13	5	11	5
# Quadruples	1	0	0	0	1	0	0	1

(c) Excess Power Generation.

FIG. 12A shows the electrical input power into the cell, and FIG. 12B shows the temperatures of the Pd cathode and Pt anode as a function of time for the D_2 cell in experiment #2. The D/Pd loading ratio for this experiment was shown in FIG. 9A. The curves shown in FIGS. 12A and 12B relate to the time interval in FIG. 9A from 15,430 to 16,030 minutes.

FIG. 12A shows that the electrical input power to the cell increased steadily with time. From FIG. 12B it can be seen that the temperature of the platinum anode stayed constant at 26.84°C during the entire time period of 600 minutes. However, the temperature of the Pd cathode showed a relatively constant value of 26.7°C only in the first 370 minutes of the time period shown. The relatively sudden temperature excursion of the Pd cathode from 26.7°C to 27.7°C followed by less elevated temperatures in the subsequent 70 minutes represents an increase in temperature which can not be explained on the basis of the smoothly rising electrical input power. On the basis of a temperature-power input calibration performed on the cell, the temperature excursion in FIG. 12B corresponds to an excess power excursion with a peak value in excess of 10W, representing a 187 times increase over the electrical input power. The excess energy produced during this power excursion amounts to approximately 5×10^4 Joules. Operation of the thermistor was verified as correct after

the conclusion of the experiment. The cell, however, was not set up to do precise calorimetry, and therefore the origin of the relatively sudden temperature excursion is uncertain.

4. Conclusions.

When D/Pd ratios in the vicinity of 1 are obtained, we have observed tritium generation on four out of four D_2 cells, whereas none of the four H_2 control cells showed any evidence for tritium generation. As we performed total tritium analysis on electrolyte, electrode, and gas before and after each experiment, and as the cells were hermetically sealed, we conclude that the tritium can only have been generated by nuclear phenomena in the deuterium-loaded palladium during the experiment.

The total tritium enhancement in the D_2 cells amounted to factors as high as 50. The total amount of tritium generated was between 4.3×10^{10} and 1.1×10^{11} T atoms/cm^2 in typically 7 days. This corresponds to an average tritium generation rate from 5.8×10^4 to 2.0×10^5 T atoms/cm^2/sec. Neutron generation has also been observed in these experiments. However, the neutron levels were fairly small, amounting on very rare occasions to 4 neutrons counted in a time frame of less than 320 μsec. In one of the four D_2 cells studied, we have found evidence for a temperature excursion lasting approximately 70 minutes with excess power values in excess of 10W and an excess energy generation of approximately 5×10^4 Joules, but the origin of the temperature excursion is uncertain.

II. APPLICATIONS

Background information regarding possible applications of nuclear reactions caused by electrolytic compression of isotopic hydrogen such as deuterium and tritium into hydrogen absorbing electrodes such as palladium or palladium alloy electrodes are described in International Application No. PCT/US90/01328 filed March

13, 1990, published on September 20, 1990 as WO 90/10935, and U.S. application Serial No. 07/641,159 filed January 14, 1991, which are incorporated herein by reference. Briefly, these references disclose that suitable metals and metal alloys for use as hydrogen absorbing electrodes are those which are capable of dissolving hydrogen in the metal lattice, such as by (i) electrolytic decomposition of hydrogen into atomic hydrogen, (ii) adsorption of the atomic hydrogen on the lattice surface, (iii) diffusion of the atoms into the lattice. The metal is also preferably capable of maintaining its structural integrity when isotopic hydrogen atoms are compressed into the metal lattice. That is, the metal lattice is capable of swelling without cracking as an increasing concentration of isotopic hydrogen atoms are compressed into the lattice. Of these, the group VIII metals, and particularly palladium, nickel, cobalt, iron, and alloys thereof, such as palladium/silver and palladium/cerium alloys, are favored, although other metals such as platinum and tantalum may also be suitable. The group VIII metals have cubic face-centered lattice structures. With diffusion of hydrogen or isotopic hydrogen atoms into the metal lattice, the lattice is able to adopt an expanded beta form which accommodates a high concentration of diffused atoms into the lattice, and effectively prevents localized strain and cracking.

From a structural standpoint, palladium alloy is superior to pure palladium. Palladium alloy can maintain dimensional stability and structural integrity during the process of electrolytic compression. Specific examples of preferred alloys having these properties are palladium (95%)-cerium (5%), and palladium (90%)- silver (10%).

The time required for charging an electrode to a saturation level generally is a function of the square of the radius of the electrode. The cycling times indicated in FIGS. 2A and 2B, for example, were selected for a 0.05

cm radius palladium electrode, and similar results for a 0.1 cm radius palladium electrode should require an expansion of the time axis by a factor of 4. However, it may also be desirable to increase the number of charging and discharging cycles for larger radius electrodes, because initially saturation typically occurs at a loading ratio of much less than one, suggesting that the loading ratio at the central region of the electrode may initially be saturated to a much smaller level than the regions of the electrode closer to the surface. Assuming a uniform saturation, which would occur if all of the isotopic hydrogen in the electrode could freely diffuse throughout the electrode, then the time for charging an electrode to a saturation level is given by the equation:

$$\text{time} \approx \frac{5\ (\text{radius})^2}{\text{diffusion coefficient}}$$

Thus, for a 0.2 cm radius palladium rod, the time for achieving saturation according to this equation is:

$$\approx \frac{5(0.2\ \text{cm})^2}{10^{-7}\ \text{cm}^2\ \text{sec}^{-1}}$$

$$\approx 20 \text{ days}$$

This formula would also give the time for achieving saturation during pre-loading of a palladium electrode with isotopic hydrogen by placing the palladium electrode in an atmosphere of isotopic hydrogen gas.

Due to the approximate nature of these computations, it is advisable to use experimental apparatus such as the apparatus in FIG. 1 to determine when saturation actually occurs for a hydrogen absorbing electrode of a particular material and a particular size. Otherwise, charging would have to be performed for a longer duration than would actually be needed in order to guarantee that the charging would be performed approximately to a level of saturation.

Electrode surface conditions can affect the flux rate of deuterium through the surface into the volume of the electrode. It is known that many metal impurities tend to migrate to the surface of a metal when heated to melt temperature for casting or annealing. For this reason, metals such as palladium which have been formed by casting or annealing may have significant platinum impurities at their surface regions, and may therefore show relatively poor charging efficiency. Conversely, a solid lattice formed by casting or annealing, followed by machining or the like to remove outer surface regions would have relatively low surface impurities. The machined lattice may be further treated, such as with abrasives, to remove possible surface contaminants from the machining process. Such methods for reducing impurities in a metal lattice are known. As noted above in the working examples, the charging rate for an electrode having a clean surface may be improved further by palladizing, and by pre-loading of the electrode with isotopic hydrogen by placing the palladized electrode in an atmosphere of isotopic hydrogen in the gas phase.

When a hydrogen absorbing electrode is used in an aqueous electrolyte, a negative voltage is applied to the electrode to charge the electrode with isotopic hydrogen; in this case the electrode is the cathode of the electrolytic cell. For some non-aqueous electrolytes such as a deuteride molten salt, however, a positive voltage must be applied to the electrode to charge the electrode with isotopic hydrogen; in this case the hydrogen absorbing electrode is the anode of the electrolytic cell. A preferred deuteride molten salt electrolyte is an eutectic LiCl-KCL molten salt saturated with lithium deuteride. Experimental results using such an electrolyte were reported by B.Y. Liaw, P-L Tao, P. Turner, and B.E. Liebert, at the Special Symposium on Cold Fusion, World

Hydrogen Energy Conference 8, Honolulu, Hawaii, July 22-27, 1990. Excess power production was reported for titanium electrodes as well as palladium electrodes. An aluminum cathode was used to receive lithium deposited by the electrochemical reaction. The excess heat, as a percentage of the total electrical power input to the cell (cell voltage x cell current) was said to be about 30% for a titanium anode 0.635 cm in diameter and 0.99 cm long after charging at 40 mA/cm^2 for two months and then charging at 240 mA/cm^2 for about 70 hours. The excess heat, as a percentage of the total electrical power input to the cell (cell voltage x cell current) was said to be about 1512% for a 0.4874 g palladium anode of irregular shape of about 0.99 cm^2 surface area. The palladium anode was charged for more than three weeks at 4 mA/cm^2 and then charged at 290 mA/cm^2 for about 30 hours, 420 mA/cm^2 for 50 hours, and then 692 mA/cm^2 for about 30 hours. The cell voltage at 692 mA/cm^2 was said to 2.453 volts, and the density of the excess heat was said to be in the range of 627 W/cm^3 Pd.

Although the working examples above used an aqueous electrolyte of 0.5 M D_2SO_4 in D_2O or H_2SO_4 in H_2O, it is not believed that the electrolyte is an important factor for obtaining consistently high loading or tritium generation. Rather, the charging and discharging durations used in the working examples indicate that the cycling procedure of the invention is the most significant aspect of the invention. Therefore the present invention should have application to a wide variety of electrolytes, including non-aqueous electrolytes such as deuteride molten salts. Moreover, the manner in which the present invention overcomes low loading saturation levels suggests that there is some kind of "memory effect" in the bulk of the palladium, which is probably related to the alpha (a) to beta (b) phase transition in the palladium. For this reason it is likely that the present invention should be useful in achieving

high loading levels of isotopic hydrogen in a wide range of hydr gen-absorbing materials that undergo phase transitions during the absorption of hydrogen, for example the group VIII metals and their alloys.

The present invention is most easily practiced by operating an electrochemical cell (e.g., the cell 20 in FIG. 1) in such a way that the cell voltage (e.g., of the palladium electrode 22 with respect to the platinum electrode 23) during discharge is constrained within voltage limits, and by alternately charging and discharging the palladium electrode in a galvanostatic (i.e, constant current) fashion.

Turning now to FIGS. 13A and 13B, there are shown graphs of the cell voltage and cell current, respectively, for another example of operation of an electrochemical cell in a galvanostatic fashion while constraining the cell voltage within voltage limits. In this example, the time scale has been shown to illustrate the charging and discharging times for consistently achieving a high loading ratio of deuterium in a 2 mm diameter palladium wire electrode so that tritium generation is consistently observed.

The cell voltage will be defined as the voltage of the palladium electrode in the cell, with the platinum electrode at a ground potential of zero volts, and the cell current will be defined as the current into the palladium electrode. For the voltage and current polarities shown in FIG. 13A and 13B, it is assumed that the electrolyte in the cell provides isotopic hydrogen cations (for example the electrolyte is an aqueous electrolyte) so that the palladium electrode becomes charged with isotopic hydrogen when the cell voltage is negative. In FIGS. 13A and 13B the voltage and current axes have been drawn with negative voltages and currents at the tops of the respective graphs and positive voltages and currents at the bottoms of the

respective graphs so that charging of the palladium electrode is generally indicated by high curves and discharging of the palladium electrode is generally indicated by low curves. More precisely, charging of the palladium electrode occurs when the curve in FIG. 13B lies above the time axis, and discharging of the palladium electrode occurs when the curve in FIG. 13B lies below the time axis. The charging and discharging, for example, is defined by the schedule listed in Table 2 below.

From FIGS. 13A and 13B, it can be seen that the palladium electrode is alternately charged and discharged in a plurality of cycles, each of the cycles including charging the palladium electrode with isotopic hydrogen to approximately a saturation level and then discharging the palladium electrode to a predetermined retention level. The palladium electrode is charged to approximately a saturation level by charging for a predetermined period of time, specified by the schedule of Table 2 below. During an initial cycle from about 0 to 4000 minutes, the palladium electrode is charged gradually by increasing the cell current in a step-wise fashion with steps of -10, -20, -30, -40, and -50 mA/cm^2.

The charging of the palladium electrode is limited so that voltage of the cell is limited to a threshold V_{NTH} to limit evolution of hydrogen gas at the palladium electrode. In practice, the desired threshold V_{NTH} is most easily established experimentally by operating the cell potentiostatically while increasing the magnitude of the cell voltage from zero until hydrogen gas is evolved at no more than a tolerable rate. The desired threshold V_{NTH} will depend upon such factors as the conductivity of the electrolyte, the gas pressure in the cell, the hydrogen over-potential of the palladium electrode, and the ability of hydrogen gas bubbles forming at the surface of the palladium electrode to become dislodged from the surface of

the electrode and rise to the surface of the electrolyte so as not to substantially interfere with the flow of electrical current in the cell.

As shown in FIG. 13B, the charging for each cycle is performed up to a maximum rate that is decreased for

TABLE 2
CELL CURRENT CYCLING SCHEDULE

INDEX	DURATION	PROGRAMMED CURRENT
0	0 min	0 mA/cm^2
1	900 min	-10 mA/cm^2
2	900 min	-20 mA/cm^2
3	900 min	-30 mA/cm^2
4	900 min	-40 mA/cm^2
5	900 min	-50 mA/cm^2
6	130 min (maximum)	30 mA/cm^2
7	130 min (maximum)	10 mA/cm^2
8	130 min (maximum)	5 mA/cm^2
9	900 min	-10 mA/cm^2
10	900 min	-20 mA/cm^2
11	130 min (maximum)	30 mA/cm^2
12	130 min (maximum)	10 mA/cm^2
13	130 min (maximum)	5 mA/cm^2
14	1500 min	-10 mA/cm^2
15	130 min (maximum)	30 mA/cm^2
16	130 min (maximum)	10 mA/cm^2
17	130 min (maximum)	5 mA/cm^2
18	1500 min	-10 mA/cm^2
19	130 min (maximum)	30 mA/cm^2
20	130 min (maximum)	10 mA/cm^2
21	130 min (maximum)	5 mA/cm^2
22	1500 min	-10 mA/cm^2
23	130 min (maximum)	30 mA/cm^2
24	130 min (maximum)	10 mA/cm^2
25	130 min (maximum)	5 mA/cm^2
26	900 min	-10 mA/cm^2
27	900 min	-20 mA/cm^2
28	900 min	-30 mA/cm^2
29	900 min	-40 mA/cm^2
30	900 min	-50 mA/cm^2
31	MAXTIME	-60 mA/cm^2

subsequent cycles following an initial cycle. The initial cycle has a maximum charging rate of -50 mA/cm^2, a second cycle has a maximum charging rate of -20 mA/cm^2, a third cycle has a maximum charging rate of -10 mA/cm^2, a fourth cycle has a maximum charging rate of -10 mA/cm^2, a fifth cycle has a maximum charging rate of -10mA/cm^2, and a sixth cycle has a maximum charging rate of -10 mA/cm^2. After the fifth cycle, the palladium electrode is charged up to a high maximum rate, preferably up to a current at which the voltage threshold V_{NTH} is reached, to initiate nuclear reactions.

It is possible that a loaded electrode might be subjected to changing conditions over a period of time so that its loading ratio might decrease. A prolonged temperature excursion, for example, might cause deuterium to diffuse out of a palladium electrode, causing nuclear reactions in the electrode to stop. It this situation it would be desirable to restore the palladium electrode to a high degree of loading by repeating cycles of the cell current schedule beginning with the discharging of the palladium electrode at a point in the schedule following the initial charging of the palladium electrode. In FIG. 13B, this point is at a time of 4500 minutes, when the cell current is switched abruptly to a discharge current of 30 mA/cm^2, corresponding to the beginning of the entry in Table 2 having an index value of 6.

As shown in FIG. 13A, the discharging is limited so that the voltage of the cell during the discharging is limited to a predetermined cell voltage threshold V_{PTH}. For an aqueous electrolyte, the cell voltage threshold V_{PTH} preferably is selected to be a point just below a voltage at which evolution of oxygen gas at the palladium electrode occurs. For an electrolyte of 0.5 M D_2SO_4 in D_2O and for atmospheric pressure and room temperature, for example, the cell voltage threshold V_{PTH} is 0.8 volts. Moreover, the

palladium electrode is discharged to a predetermined retention level by discharging until the cell voltage threshold V_{PTH} is reached at a predetermined discharge current. As shown by FIG. 13A and FIG. 13B in combination, each charging phase of a cycle is abruptly terminated and the discharge phase begins abruptly and immediately after the charging phase. The discharging phase during each cycle is performed at a maximum rate of 30 mA/cm^2 immediately after the charging phase of the cycle, and thereafter the rate of discharging is decreased to 10 and then 5 mA/cm^2 during the cycle. In particular, the rate of discharging is decreased during each cycle when the cell voltage reaches the cell voltage threshold V_{PTH}. The discharging phase of each cycle is terminated to begin the charging phase of the next cycle when the cell voltage threshold V_{PTH} is reached at the 5 mA/cm^2 discharge current.

Turning now to FIG. 14, there is shown a block diagram of a system including a battery of cells 100 and a digital computer 101 for cycling current to a palladium electrode 102, 103 in each of the cells. The battery of cells 100, for example, has a planar geometry and includes platinum foil electrodes 104, 105, 106 that serve as cell separators and are all connected to ground potential. The platinum electrodes 104, 105, 106 are separated from the palladium electrodes 102, 103 by separator sheets 107, 108 of microporous material such as microporous plastic.

To cycle the current to each palladium electrode 102, 103, each palladium electrode is connected to a respective cell power supply 111, 112. The cell power supplies are controlled by a programmable digital computer 113. In particular, a data bus 116 interconnects the computer 113 and the power supplies for the exchange of control data, and an address bus 115 interconnects the computer and the power supplies 111, 112 to permit the computer to select a particular one of the power supplies

for the exchange of data. The cell power supplies 111, 112 are further described below with reference to FIG. 16.

The digital computer 113 is programmed, as further described below with reference to FIGS. 17 to 20, to achieve a high degree of loading of deuterium in each of the palladium electrodes 102, 103 by controlling the cell power supplies 111, 112 in accordance with a cell current schedule 117. The cell current schedule, for example, is a table of cell current set points and time durations in computer memory in the format of Table 2 above. The computer 113 also has a real-time clock 118 that is used in connection with the cell current schedule 117 to make changes to the settings of the power supplies 111, 112 at the scheduled times.

To monitor the performance of the battery 100, the digital computer has an analog-to-digital converter 119 for periodically sampling the cell voltage and the temperatures of the electrodes in each cell. To sample the value of a selected parameter, the digital computer 113 places a predetermined address on the address bus 115. The address is decoded by an address decoder 121, which enables a data register 122 to accept a data code indicating the selected parameter. The code is fed to an analog multiplexer 123, which connects an input of the analog-to-digital converter 119 to a selected palladium electrode 102, 103 to sample the voltage of a cell, or to sample the output of a selected thermistor amplifier 124, 125, 126, 127. After a predetermined conversion time interval required by the analog-to-digital converter 119, the computer 113 reads a digital sample from the analog-to-digital converter by placing an address on the address bus 115. The address is decoded by the address decoder 121, which enables a bus driver 128 to transmit the digital sample over the data bus 116 to the computer 113.

Turning now to FIG. 15, there is shown a schematic

diagram of a conventional thermistor amplifier 127. A thermistor 131 associated with the amplifier 127 is a component of a bridge circuit also including resistors 132 and 133 of approximately equal resistance R_1, and a variable resistor 134. The bridge is energized by a regulated voltage $+V_R$. The output of the bridge is fed to an operational amplifier 135. Resistors 138, 139, 140 and 141 set the gain of the operational amplifier 135. It is known that the performance of the circuit is optimized when the resistance R_1 is equal to the nominal resistance of the thermistor 131, the resistors 138 and 139 have the same resistance R_2, and the resistors 140 and 141 have the same resistance R_3. The gain of the amplifier 135 is given by the ratio R_3/R_2. The variable resistor 134 is adjusted to null the output of the bridge at a nominal temperature, and a null output of the bridge is indicated by a zero (mid-range) output from the amplifier 135.

Turning now to FIG. 16, there is shown a schematic diagram of the cell power supply 111. The cell voltage is sensed by a pair of operational amplifiers 151, 152 (such as part No. 741). The cell current is supplied by a power driver 154 and is sensed by a series resistance 153. The power driver may have essentially the same construction as the output stage of a direct-coupled audio amplifier, and for cell currents up to about an ampere, an audio amplifier integrated circuit could be used, such as part No. SN76023 or CA3132EM.

The operational amplifier 151 compares the cell voltage to the positive threshold V_{PTH}, and when the cell voltage reaches the positive threshold, then the operational amplifier 151 prevents any further rise in the cell voltage by clamping the input to the power driver 154. For this purpose, the output of the operational amplifier 151 is fed back to the input of the power driver 154 through a directional diode 155 and a pnp transistor 156.

The pnp transistor is used so that the clamping current can be sensed by a resistor 157 and an npn transistor 158. The output of the npn transistor 158 is level-shifted by a pnp transistor 159 to ground and +Vs (such as 5 volts) to provide a logic signal "V_{PTH} SENSE" that is transmitted by a bus driver 160 to the computer (113 in FIG. 14) to indicate when the cell voltage reaches the positive threshold V_{PTH}. The bus driver 160 is enabled when the computer addresses an address decoder 161 to monitor the status of the power supply 111.

In a similar fashion, the operational amplifier 152 compares the cell voltage to the negative threshold V_{NTH}, and when the cell voltage reaches the negative threshold, then the operational amplifier 152 prevents any further decrease in the cell voltage by clamping the input to the power driver 154. For this purpose, the output of the operational amplifier 152 is fed back to the input of the power driver 154 through a directional diode 162 and an npn transistor 163. The npn transistor 163 is used so that the clamping current can be sensed by a resistor 164 and a pnp transistor 165. Transistor 165 provides a logic signal "V_{NTH} SENSE" that is fed back by the bus driver 160 to the computer (113 in FIG. 14) to indicate when the cell voltage reaches the negative threshold V_{NTH}.

So long as the cell voltage is within the positive and negative thresholds, the cell current is regulated to a selected value in response to a comparison of the voltage across the current sensing resistor 153 to a set-point value. To adjust the cell current, the computer (113 in FIG. 14) addresses the address decoder 161 to enable a data register 171 to receive a data code indicating a current set-point. The data code is fed to a digital-to-analog converter 172, such as an "R/2R ladder network", that provides a voltage ranging from -Vs to +Vs (for example from -5 volts to + 5 volts) depending on the value of the

data code. For an 8-bit data code, for example, a code of 00 hexadecimal provides a voltage of -Vs, a code of 7F hexadecimal provides a voltage of -Vs/255, a code of 80 hexadecimal provides a voltage of +Vs/255, and a code of FF hexadecimal provides a voltage of +Vs. The output of the digital-to-analog converter is then fed through a variable resistor 173 and a resistor 174 to the negative input of an operational amplifier 190 that compares the control voltage to a voltage indicating the cell current.

The voltage indicating the cell current is provided by an operational amplifier 176 that works in conjunction with resistors 177, 178, 179, 180, 181 and 182 to provide a voltage referenced to ground indicating the current through the current sensing resistor 153. In other words, the amplifier functions as a differential amplifier to amplify the voltage difference across current sensing resistor 153 without significantly responding to any variation in cell voltage. This condition can be achieved by selecting resistors 177 and 178 to have approximately the same value R_4, and selecting resistor 181 and the total resistance of resistor 179 and resistor 180 to have the same value R_5. The gain of the amplifier 176 is set by the ratio R_5/R_4, and this ratio should be selected, along with the value of the current sensing resistor 153, so that the output of the amplifier 176 swings within its linear range when the cell current swings over the desired range of cell current.

The operational amplifier 190 drives the power driver 154 through a resistor 192 that is needed for the clamping function described above. Associated with the operational amplifier 190 is a capacitor 195 that sets the response time of the amplifier 190. The response time is the product of the capacitance C and the resistance at the negative input of the amplifier 190. The response time, for example, is about 15 milliseconds, and it ensures

stability of current control by providing a "dominant pole" in the feedback loop consisting of the amplifier 190, the power driver 154, and the amplifier 176.

As shown in FIG. 16, the positive threshold V_{PTH} and the negative threshold V_{NTH} are established by potentiometers 195, 196. Alternatively, these thresholds could be established by respective analog-to-digital converters (not shown) to provide computer adjustment of the thresholds.

Suggested component values for the components in the power supply 111 in FIG. 16 are as follows:

Resistor:	Value:
153	5.0 ohms (for I_{CELL} = -127 to +128 mA)
157	4.7 k ohms
164	4.7 k ohms
166	10 k ohms
167	4.7 K ohms
168	4.7 K ohms
169	4.7 K ohms
173	3.3 K ohms
174	18.0 K ohms
177	10.0 K ohms
178	10.0 K ohms
179	38 K ohms
180	4.7 K ohms
181	40 K ohms
182	10 K ohms
194	10 K ohms
195	2.2 microfarads

The power supply circuit in FIG. 16 is calibrated by connecting the power supply cell terminals 197, 198 to a voltmeter 199, an adjustable load resistor 200, and an ammeter 201. The variable resistors 173, 179, 180, 195 and 196 are set to mid-range positions. Then a data code (such as 80 hexadecimal) is transmitted by the computer (113 in FIG. 14) to the digital-to-analog converter 172 to set a minimum cell current. Next, the load resistor 200 is adjusted to a minimum resistance, and the resistor 182 is adjusted to obtain a zero current reading by the ammeter 201.

The power supply circuit in FIG. 16 is somewhat unusual in that the current sensing resistor 153 does not have one of its terminal connected to ground. This permits independent current sensing to a respective palladium electrode in the battery of cells 100 having the platinum electrodes all connected together to ground, which would be desirable in a power-generating reactor. For the circuit in FIG. 1, the fact that the current sensing resistor 153 does not have one of its terminals connected to ground causes some variation in the output of the amplifier 176 with the cell voltage, due to so-called "common mode" signal amplification, unless resistor 180 is adjusted to null out the common mode. To null out the common mode (CM), a data code of 81 hexadecimal (representing -1 mA, assuming 1 mA steps) is transmitted by the computer to the digital-to-analog converter. Then the actual current reading indicated by the ammeter 201 is noted. Next, the load resistance 200 is increased, until the voltmeter 199 reads 2 volts. The current reading indicated by the ammeter 201 is observed, and if it has changed, then the resistor 180 is adjusted to bring the reading back to its original value.

To calibrate the power supply for a "full scale" value, the load resistance 200 is set back to a minimum

value, and then a data code of FF hexadecimal (representing 127 mA, assuming 1 mA steps) is transmitted by the computer to the digital-to-analog converter 172. Then the resistor 173 is adjusted to obtain precisely the desired full-scale value. The resistor 173 is intended to have a rather narrow adjustment range in order to provide a precise adjustment. If it is desired to obtain a large change in the full-scale value, this should be done by changing the current sensing resistance 153. A switch (not shown) could be provided to select one of a number of precision current sensing resistors (not shown) for different respective current ranges, as is the common practice in power supplies and current measuring instruments.

The positive and negative thresholds (V_{PTH} and V_{NTH}) can be adjusted approximately by connecting a voltmeter (not shown) to the taps of the respective potentiometers 195, 196. A more precise adjustment for a particular cell current set-point could be made by transmitting the a code for the current set-point from the computer to the digital-to-analog converter 172, and then increasing the load resistance 200 until the voltage indicated by the voltmeter 199 becomes limited to a respective one of the positive or negative voltage thresholds. The potentiometer 195, 196 for the respective threshold can then be adjusted to obtain a desired voltage threshold indication by the voltmeter 199.

It should now be apparent that the digital computer 113 in FIG. 14 can be programmed to automatically perform the method of the present invention upon each of the palladium electrodes in the battery 107 by the transfer of data between the computer and the power supplies 111, 112. The programming, for example, includes an executive program 200 in FIG. 17 that is started to begin loading of the palladium electrodes, an interrupt routine 220 in FIG. 18 that is executed once every minute in response to an

interrupt from the real-time clock (118 in FIG. 14), and a routine 230 in FIG. 19 that is called by the interrupt routine once for each cell.

Turning now to FIG. 17, in the first step 201 of the executive program 200, the computer clears values for the parameters of each cell. These parameters include the next time that the cell current needs to be updated (CELL_TIME(i)), the step in the cell current cycling schedule that the cell is presently at (INDEX(i)), the temperature of the palladium electrode in the cell (TEMPC(i)), the cell voltage (VOLT(i)), and the cell current set-point (CURRENT(i)). Next, in step 203, the cell current set-point (of zero mA) is transmitted to each of the cell power supplies. Then, in step 203, the cell power supplies are energized. It is assumed, for example, that the address decoder 161, bus driver 160 and data register 171 in each cell power supply 111 (FIG. 16) are powered by the computer, so that when the cell power supplies are turned on, for example by the computer energizing a latching relay, the cell voltage and cell current for each of the cells will initially have zero values.

In step 204, the value of a variable "BEGIN_TIME" is set to the value of the present time indicated by the real-time clock (118 in FIG. 14). Next in step 205 a cell data matrix is displayed by the computer. This cell data matrix, for example, includes the values of the schedule index, temperatures, voltage, and current set-point for each cell. Then in step 204 the sample timer interrupt is enabled, so that the sample timer interrupt routine 220 of FIG. 18 is periodically executed, for example, once every minute.

In step 207, the computer operator may enter an "escape" command to exit the executive program 200 and enter the operating system, for example, to run other

programs. Otherwise, in step 208 the executive program may monitor the performance of the cells, for example, by searching for cells having anomalous temperature excursions, or possibly by monitoring other data collected about the cells, such as data inputted to the computer about analysis of tritium content of the electrolyte in the respective cells, or data inputted to the computer about neutrons or x-rays detected from the respective cells. In step 209, at a certain time after the loading cycle is completed for a cell (as indicated by the schedule index for the cell reaching a predetermined maximum value), the computer may formulate a judgement about the performance of the cell. When the computer decides that the performance of the cell is poor, then in step 210 the computer may attempt to restore the loading of the cell to a high loading ratio, by repeating the cycling schedule for the cell, beginning with discharging of the electrode at the point in the schedule following the initial charging of the cell at a high rate. This is done in step 210 by calling a restoration routine 250 described further below with reference to FIG. 20.

Turning now to FIG. 18, there is shown a flowchart of the sample timer interrupt routine 220. In the first step 221, the value of a variable "ELAPSED_TIME" is computed by subtracting the value of the variable "BEGIN_TIME" from the present time indicated by the real-time clock (118 in FIG. 14). Next in step 222 the present time and the elapsed time are recorded in a log file and displayed to the computer operator. Then in step 223, for each cell, the cell parameters are sampled, recorded and displayed. In particular, the cell voltage, cell temperatures, and any indications of the voltage limit thresholds being exceeded, are sampled, recorded and displayed. Then in step 224, the cell current set-point for each cell is recorded and displayed. Finally, in step

225, the cycle routine 230 of FIG. 19 is called for each cell possibly to update the cell current set-point.

Turning now to FIG. 19, there is shown a flowchart of the cycle routine 230. In the first step 231, the value of the scheduled current for the index value of the cell is compared to zero to determine whether the cell is being charged. If the cell is being charged, then in step 232 the value of the variable "ELAPSED_TIME" is compared to the value of the cell time for the cell; when the elapsed time is equal to or greater than the cell time for the cell, then the cell current is updated in accordance with the cell current schedule. For this purpose, in step 233 the index for the cell is compared to a predetermined maximum value to determine whether the cycling for the cell has reached the end of the schedule. If not, then the index for the cell is incremented in step 234.

In step 235, the schedule is indexed with the index for the cell in order to obtain the scheduled cell current set-point, and the cell current set-point is transmitted to the respective power supply for the cell. Finally, in step 236 the cell time for the next update of the cell current set-point is computed as the sum of the elapsed time and the duration obtained by indexing the cell current schedule with the index for the cell.

It should be apparent that when a cell is being charged, it will be updated only at the next scheduled time. This is done because the cell parameters monitored by the computer 133 in FIG. 14 cannot precisely indicate the effectiveness of charging a particular cell at a particular current level. Moreover, charging a cell for a period of time that is somewhat longer than necessary would tend to possibly increase the loading ratio, and would not decrease the loading ratio. In contrast, when a cell is discharged during a step in the schedule, it is rather easy for the computer to determine whether a particular cell has

been discharged to a predetermined retention level, and discharging the cell for a period of time that is longer than necessary might tend to decrease the loading ratio. Therefore, in step 237, a cell is advanced immediately to the next step in the cell current schedule when the voltage threshold indicates that a predetermined level of discharging has been achieved at the present level of discharge current. For an aqueous solution, the proper voltage threshold is the positive voltage threshold, and the logic signal V_{PTH} SENSE from the power supply of the cell indicates whether the positive voltage threshold has been reached. Otherwise, in step 238, the elapsed time is compared to the cell time for the cell. The elapsed time should not normally be equal to or greater than the cell time for the cell, because the durations for the discharge steps in the cell current schedule should be selected so that the predetermined level of discharging is normally reached before the elapsed time reaches the cell time. Otherwise, as indicated in step 239, the cell is indicated as having a discharge problem, and the cell current is updated in steps 233-236 in accordance with the cell current schedule.

Turning now to FIG. 20, there is shown a flowchart 250 of a routine for restoring a specified cell to a high state of loading. In the first step 251, the sample timer interrupt is disabled. Next in step 252, the value of the schedule index for the cell is set to 5, and the current time for the cell is set to the elapsed time. Finally, in step 253 the sample timer interrupt is enabled. Therefore, at the next sampling time, the index for the cell will be advanced to 6, and the current set-point for the cell will be updated to begin discharging the cell at a high rate.

In view of the above, there has been described a method for achieving a high loading ratio of isotopic hydrogen in hydrogen absorbing electrodes. The procedure

overcomes what appears to be a kind of "memory effect" inherent in palladium and probably other hydrogen absorbing materials that undergo phase transitions during the absorption of hydrogen, such as the group VIII metals and their alloys. The procedure has been successful in 4 out of 4 experiments for consistent reproduction of a high loading ratio of deuterium in palladium in the vicinity of 1:1, and consistent reproduction of tritium generation. The procedure can be easily carried out automatically by a digital computer, and the digital computer can easily control a large number of cells. The procedure therefore can be applied immediately to banks of cells for experimental purposes. Moreover, it is anticipated that in a nuclear reactor having a multiplicity of deuterium absorbing electrodes, each of the electrodes will be independently loaded and possibly restored to a high degree of loading numerous times during operation of the reactor under computer control in accordance with the invention.

What is claimed is:

Claims

1. A method of obtaining a high degree of loading of isotopic hydrogen in an electrode of hydrogen absorbing material, said electrode being part of an electrolytic cell having an electrolyte providing a source of said isotopic hydrogen, said method comprising the steps of alternately charging and discharging the electrode in a plurality of cycles, each of said cycles including charging the electrode with isotopic hydrogen to approximately a saturation level and then discharging the electrode to a predetermined retention level.

2. The method as claimed in claim 1, wherein the electrode is charged to approximately a saturation level by charging for a predetermined period of time.

3. The method as claimed in claim 2, wherein charging of the electrode is limited so that voltage of the cell is limited to limit evolution of hydrogen gas at the electrode.

4. The method as claimed in claim 1, wherein charging for each cycle is performed up to a maximum rate that is decreased for subsequent cycles following an initial cycle.

5. The method as claimed in claim 4, further comprising the steps of restoring the electrode to a high degree of loading by repeating cycles of said charging and discharging, beginning with discharging of the electrode.

6. The method as claimed in claim 5, wherein the beginning of the discharging occurs at a point in a predefined control schedule following an initial charging of the electrode at a high rate.

7. The method as claimed in claim 1, wherein the discharging is limited so that the voltage of the cell during the discharging is limited to a predetermined cell voltage threshold.

8. The method as claimed in claim 7, wherein the electrolyte is an aqueous electrolyte, and the predetermined cell voltage threshold is selected to be a point just below a voltage at which evolution of oxygen gas at the electrode occurs.

9. The method as claimed in claim 1, wherein the electrode is discharged to a predetermined retention level by discharging until a predetermined cell voltage threshold is reached at a predetermined discharge current.

10. The method as claimed in claim 9, wherein the discharging is limited so that the cell voltage during the discharging is limited to said predetermined cell voltage.

11. The method as claimed in claim 1, wherein the discharging during each cycle is performed abruptly immediately after the charging during said each cycle.

12. The method as claimed in claim 11, wherein the discharging during each cycle is performed at a maximum rate immediately after the charging during said each cycle, and thereafter the rate of discharging is decreased during said each cycle.

13. The method as claimed in claim 12, wherein the discharging is limited so that the cell voltage during the discharging is limited to a predetermined cell voltage, and wherein the rate of discharging is decreased during each cycle when the cell voltage reaches said predetermined cell

voltage.

14. The method as claimed in claim 1, further comprising the step of monitoring the degree of loading of isotopic hydrogen in the electrode, and wherein the charging the electrode with isotopic hydrogen to approximately a saturation level is performed for a duration of time based upon the monitoring of the degree of loading of isotopic hydrogen in the electrode.

15. A method of obtaining a high degree of loading of isotopic hydrogen in an electrode of hydrogen absorbing material, said electrode being part of an electrolytic cell having an electrolyte providing a source of said isotopic hydrogen, said method comprising the steps of alternately charging and discharging the electrode in a plurality of cycles, each of said cycles including charging the electrode with isotopic hydrogen to approximately a saturation level and then discharging the electrode to a predetermined retention level, wherein the electrode is charged to approximately a saturation level by charging for a predetermined period of time, and wherein the discharging is limited so that the voltage of the cell during the discharging is limited to a predetermined cell voltage threshold.

16. The method as claimed in claim 15, wherein charging for each cycle is performed up to a maximum rate that is decreased for subsequent cycles following an initial cycle.

17. The method as claimed in claim 15, wherein the electrode is discharged to a predetermined retention level by discharging until the predetermined cell voltage threshold is reached at a predetermined discharge current.

18. The method as claimed in claim 15, wherein the electrolyte is an aqueous electrolyte, and the predetermined cell voltage threshold is selected to be a point just below a voltage at which evolution of oxygen gas at the electrode occurs.

19. A method of obtaining a high degree of loading of isotopic hydrogen in an electrode of hydrogen absorbing material, said electrode being part of an electrolytic cell having an electrolyte providing a source of said isotopic hydrogen, said method comprising the steps of alternately charging and discharging the electrode in a plurality of cycles, each of said cycles including charging the electrode with isotopic hydrogen to approximately a saturation level and then discharging the electrode to a predetermined retention level, wherein charging for each cycle is performed up to a maximum rate that is decreased for subsequent cycles following an initial cycle, and the discharging is limited so that the voltage of the cell during the discharging is limited to a predetermined cell voltage threshold.

20. The method as claimed in claim 19, wherein the electrolyte is an aqueous electrolyte, and the predetermined cell voltage threshold is selected to be a point just below a voltage at which evolution of oxygen gas at the electrode occurs.

21. The method as claimed in claim 19, wherein the electrode is discharged to a predetermined retention level by discharging until said predetermined cell voltage threshold is reached at a predetermined discharge current.

22. A method of obtaining a sufficiently high degree of loading of deuterium in a palladium or palladium

alloy electrode to consistently observe the generation of tritium, said electrode being part of an electrolytic cell having an electrolyte providing a source of said isotopic hydrogen, said method comprising the steps of alternately charging and discharging the electrode in a plurality of cycles, each of said cycles including charging the electrode with isotopic hydrogen to approximately a saturation level and then discharging the electrode to a predetermined retention level, wherein discharging is limited so that the voltage of the cell during the discharging is limited to a predetermined cell voltage threshold.

23. The method as claimed in claim 22, wherein charging for each cycle is performed up to a maximum rate that is decreased for subsequent cycles following an initial cycle.

24. The method as claimed in claim 22, wherein the electrode is charged to approximately a saturation level by charging for a predetermined period of time.

25. The method as claimed in claim 22, wherein the electrode is discharged to a predetermined retention level by discharging until the predetermined cell voltage threshold is reached at a predetermined discharge current.

26. The method as claimed in claim 22, further comprising the step of pre-treating the electrode prior to the steps of alternately charging and discharging the electrode, where said pre-treating includes forming a thin surface layer of palladium black upon the electrode.

27. The method as claimed in claim 26, wherein said pre-treating further includes pre-loading the electrode

with isotopic hydrogen by placing the electrode in an atmosphere including isotopic hydrogen gas.

28. The method as claimed in claim 22, wherein the electrolyte is an aqueous electrolyte, and the predetermined cell voltage threshold is selected to be a point just below a voltage at which evolution of oxygen gas at the electrode occurs.

29. The method as claimed in claim 22, wherein the discharging during each cycle is performed abruptly immediately after the charging during said each cycle.

30. The method as claimed in claim 22, wherein the discharging during each cycle is performed at a maximum rate immediately after the charging during said each cycle, and thereafter the rate of discharging is decreased during said each cycle.

31. The method as claimed in claim 22, wherein charging of the electrode is limited so that voltage of the cell is limited to limit evolution of hydrogen gas at the electrode.

32. The method as claimed in claim 22, wherein the method includes at least four of said cycles.

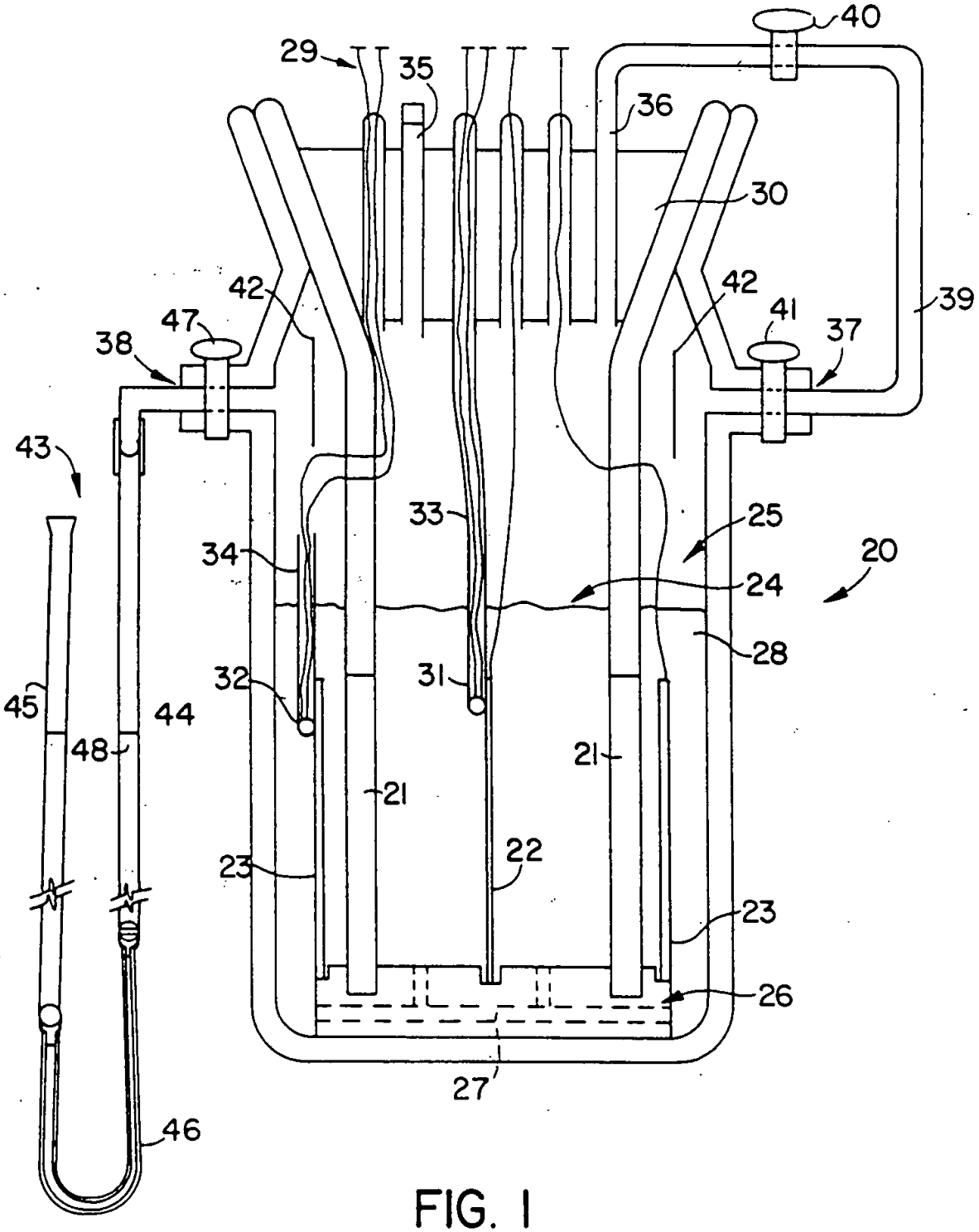
40
29
35
36
30
42
42
41
39
37
47
38
43
33
25
34
20
24
28
32
31
45
44
48
21
21
23
22
23
26
27
46

FIG. 1

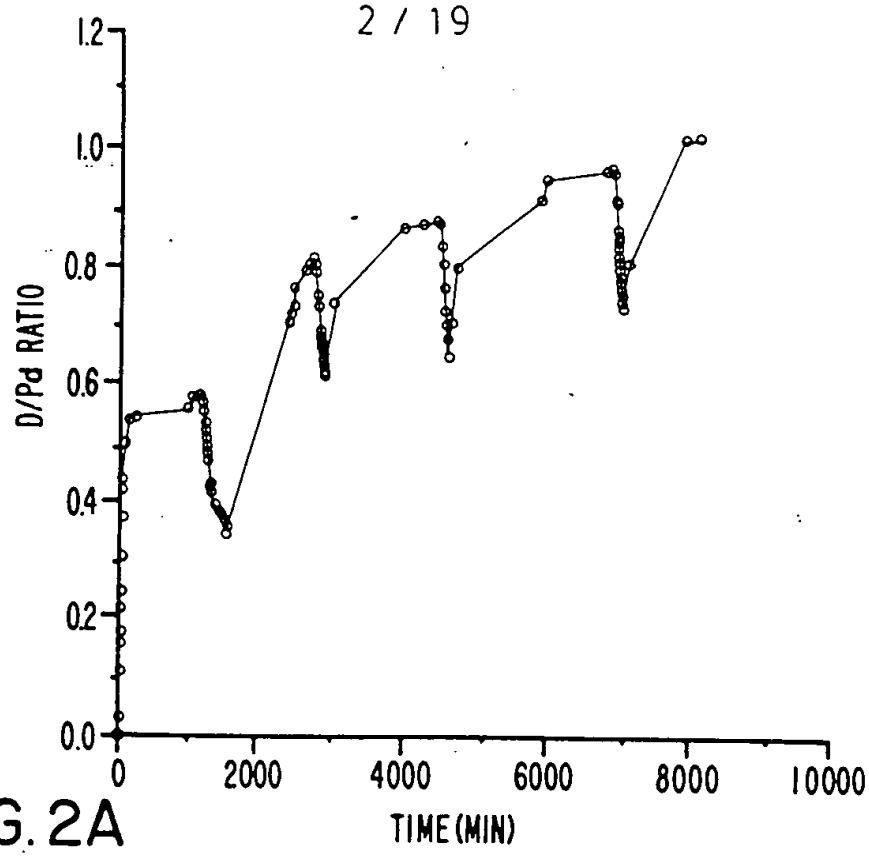
D/Pd RATIO
1.2
1.0
0.8
0.6
0.4
0.2
0.0
0
2000
4000
6000
8000
10000
TIME (MIN)

FIG. 2A

FIG. 2B

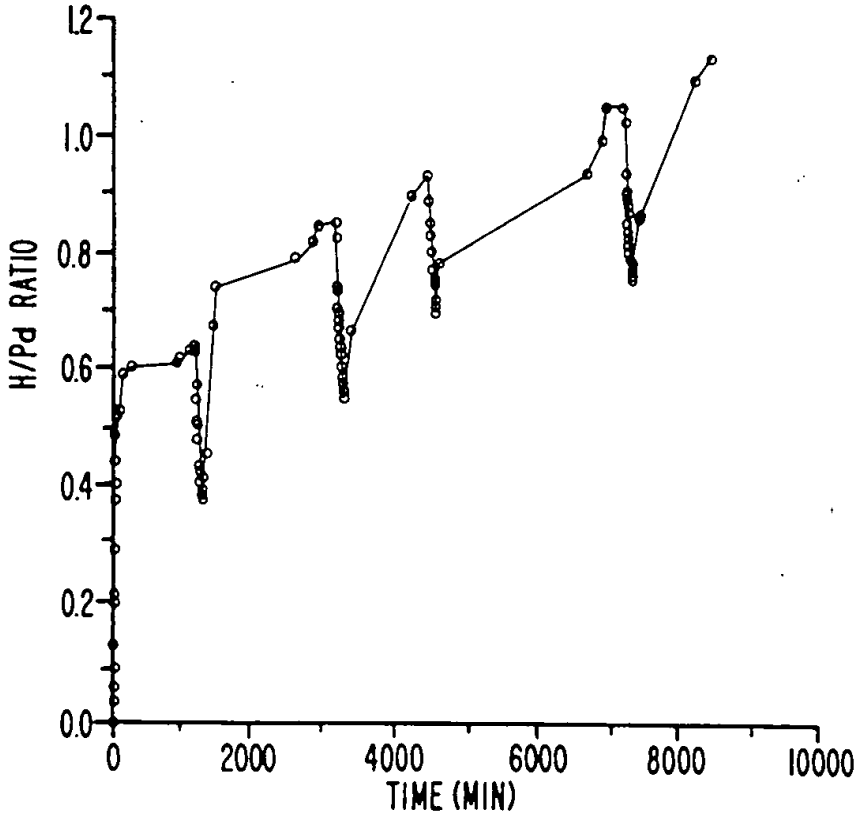
H/Pd RATIO
1.2
1.0
0.8
0.6
0.4
0.2
0.0
0
2000
4000
6000
8000
10000
TIME (MIN)

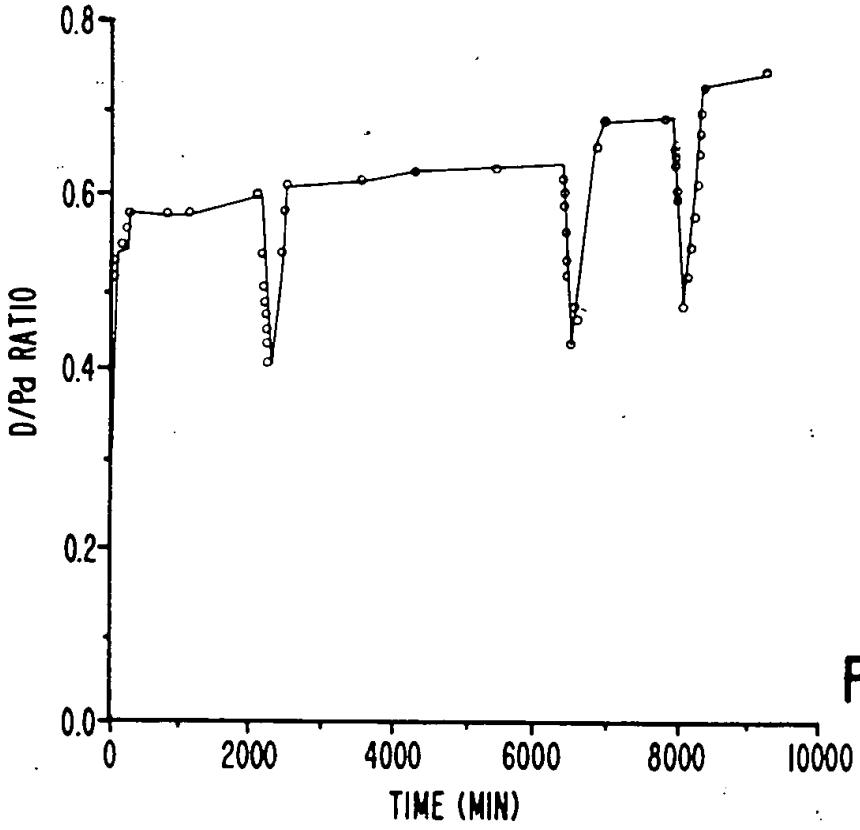
0.8
0.6
0.4
0.2
0.0
D/Pd RATIO
0
2000
4000
6000
8000
10000
TIME (MIN)

FIG. 3A

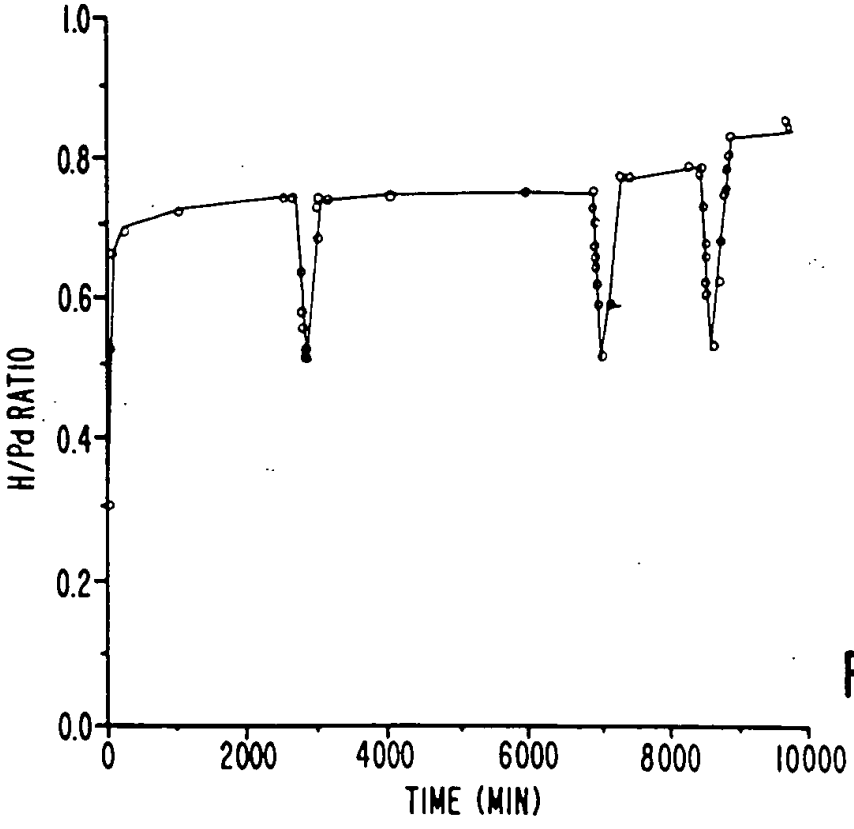
1.0
0.8
0.6
0.4
0.2
0.0
H/Pd RATIO
0
2000
4000
6000
8000
10000
TIME (MIN)

FIG. 3B

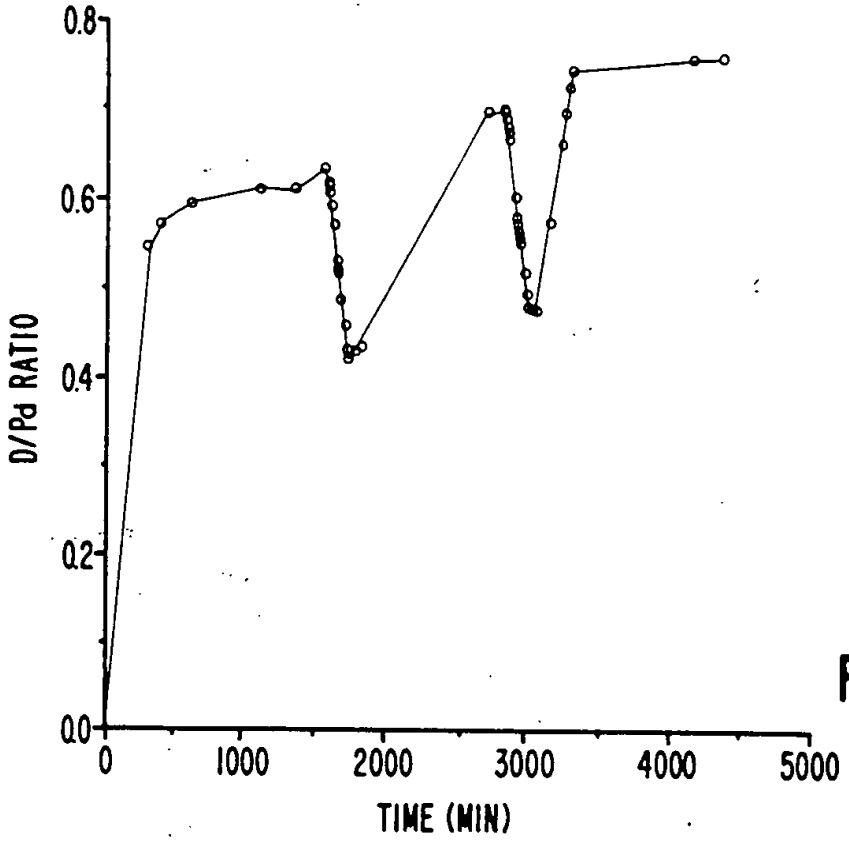
0.8
0.6
0.4
0.2
0.0
D/Pd RATIO
0
1000
2000
3000
4000
5000
TIME (MIN)

FIG. 4A

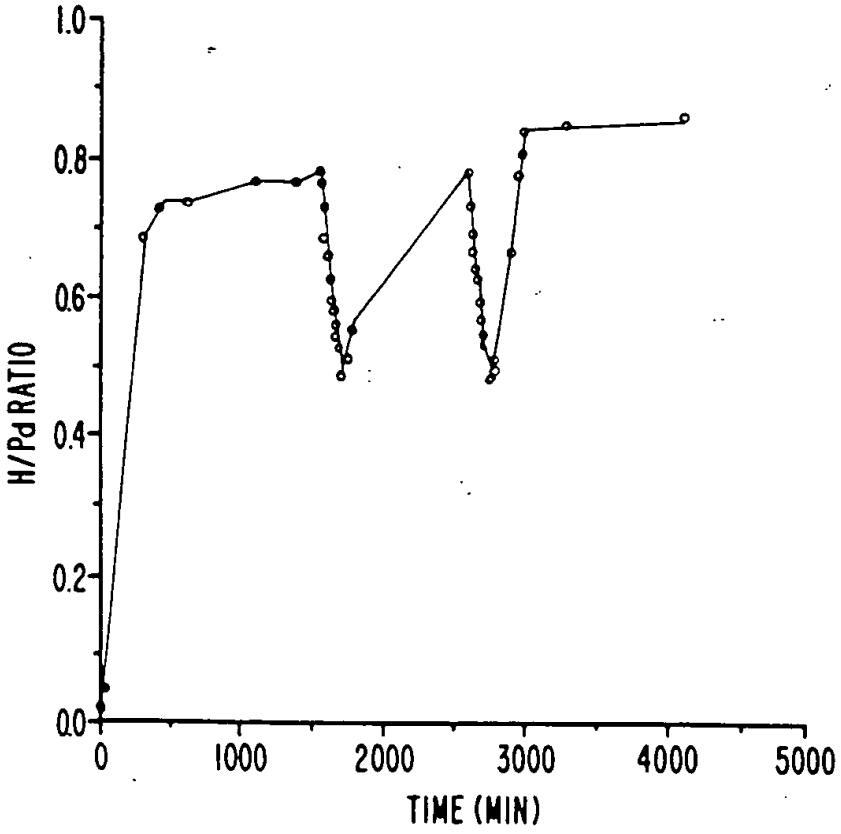
1.0
0.8
0.6
0.4
0.2
0.0
H/Pd RATIO
0
1000
2000
3000
4000
5000
TIME (MIN)

FIG. 4B

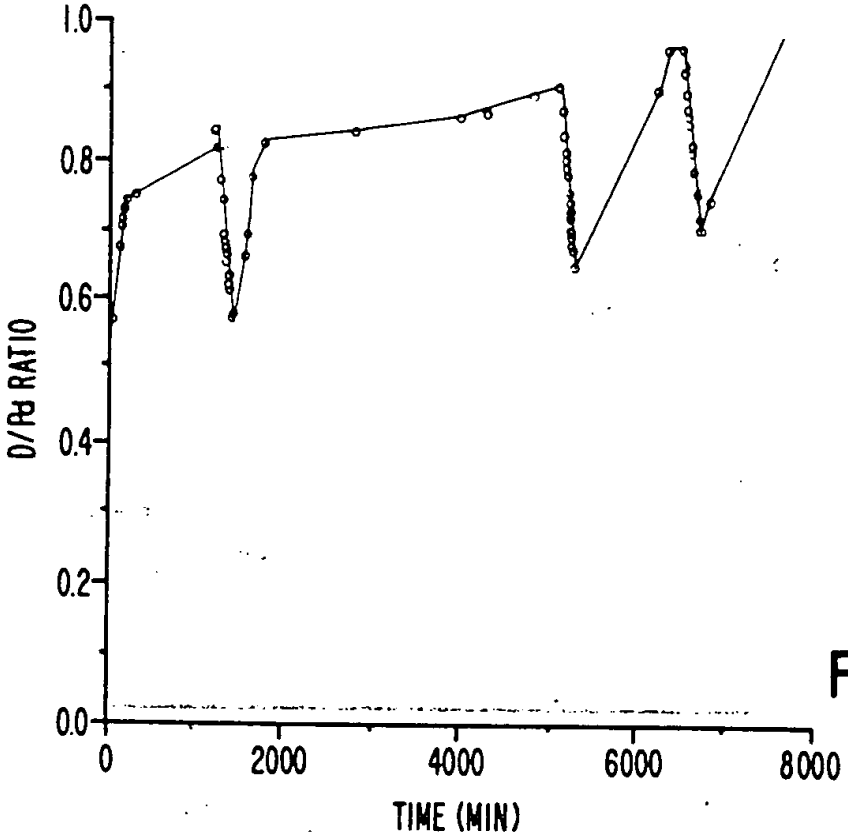
1.0
0.8
0.6
0.4
0.2
0.0
D/Pd RATIO
0
2000
4000
6000
8000
TIME (MIN)

FIG. 5A

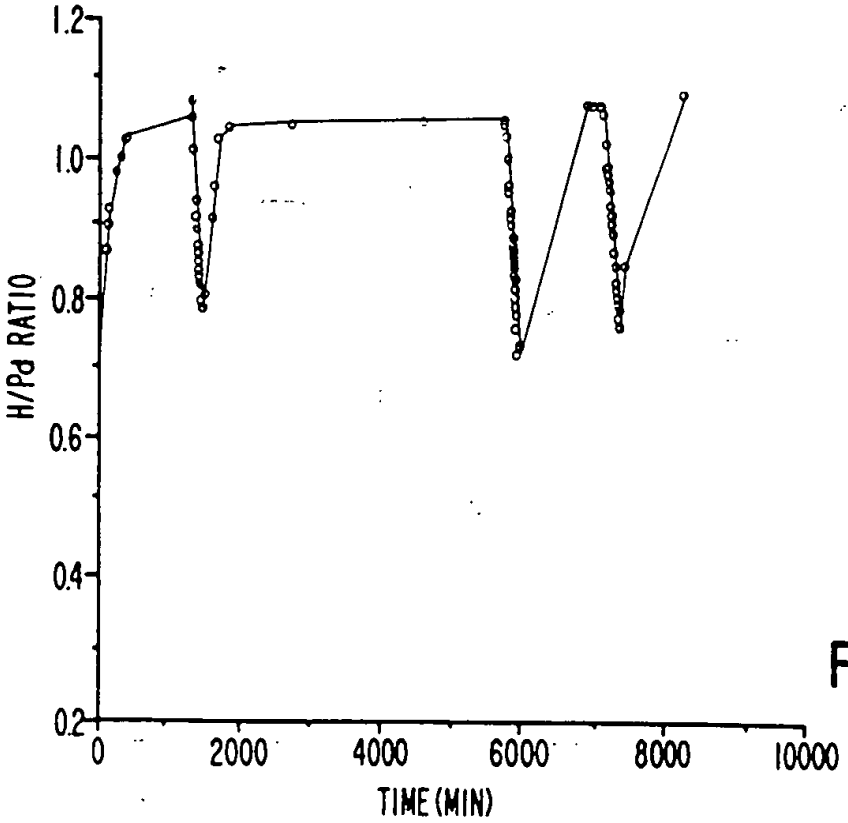
1.2
1.0
0.8
0.6
0.4
0.2
H/Pd RATIO
0
2000
4000
6000
8000
10000
TIME (MIN)

FIG. 5B

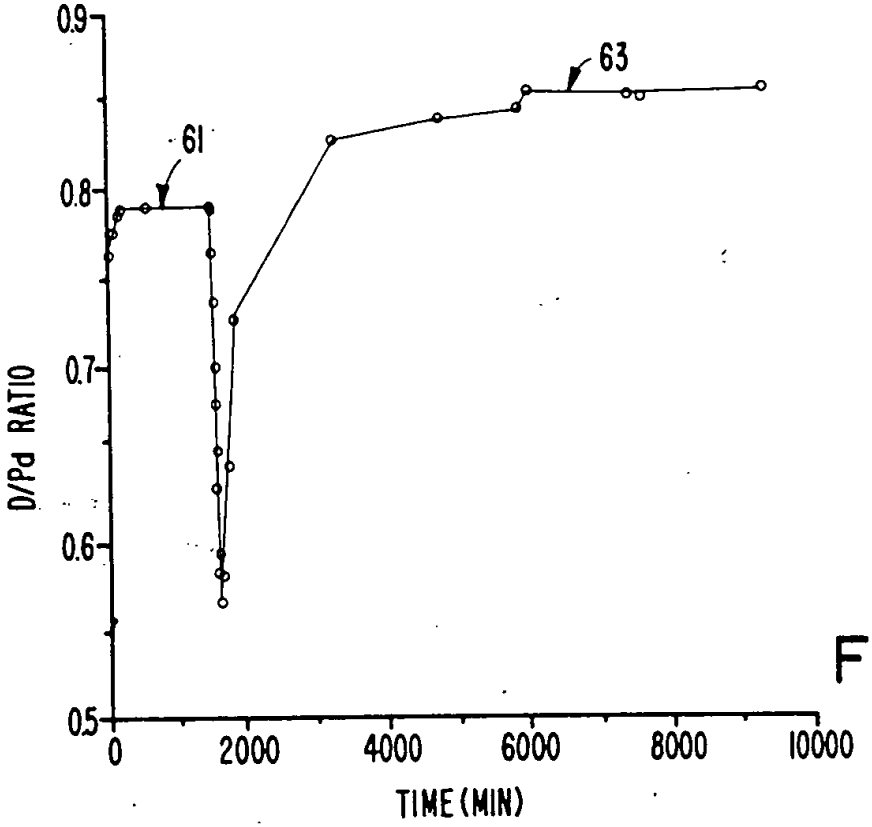
0.9
0.8
0.7
0.6
0.5
D/Pd RATIO
61
63
0
2000
4000
6000
8000
10000
TIME (MIN)

FIG. 6A

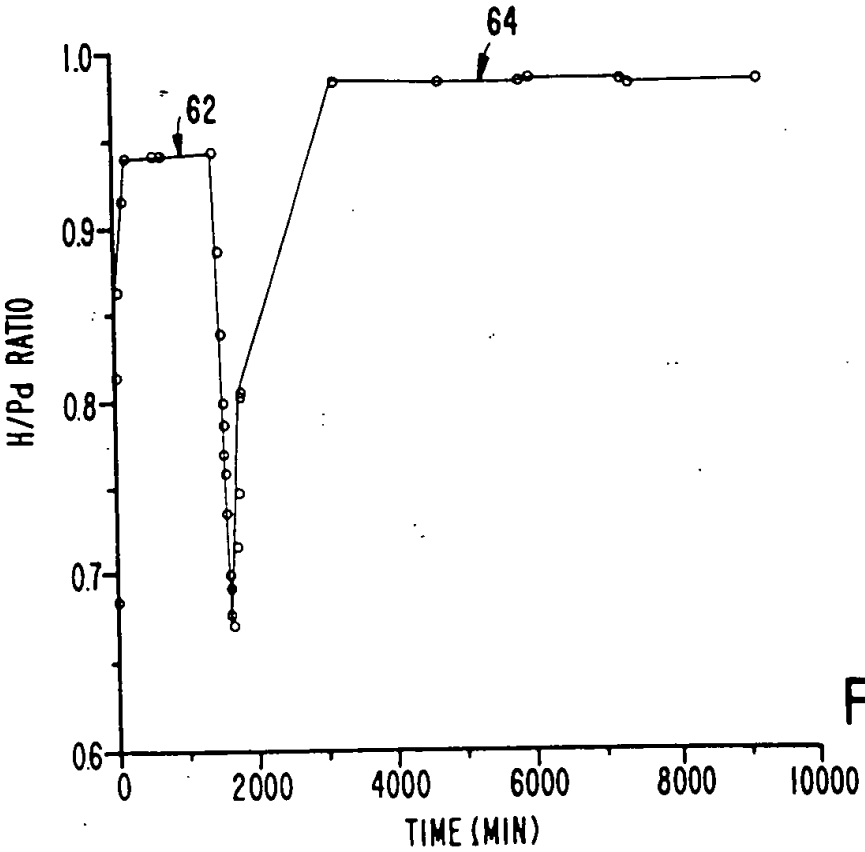
1.0
0.9
0.8
0.7
0.6
H/Pd RATIO
62
64
0
2000
4000
6000
8000
10000
TIME (MIN)

FIG. 6B

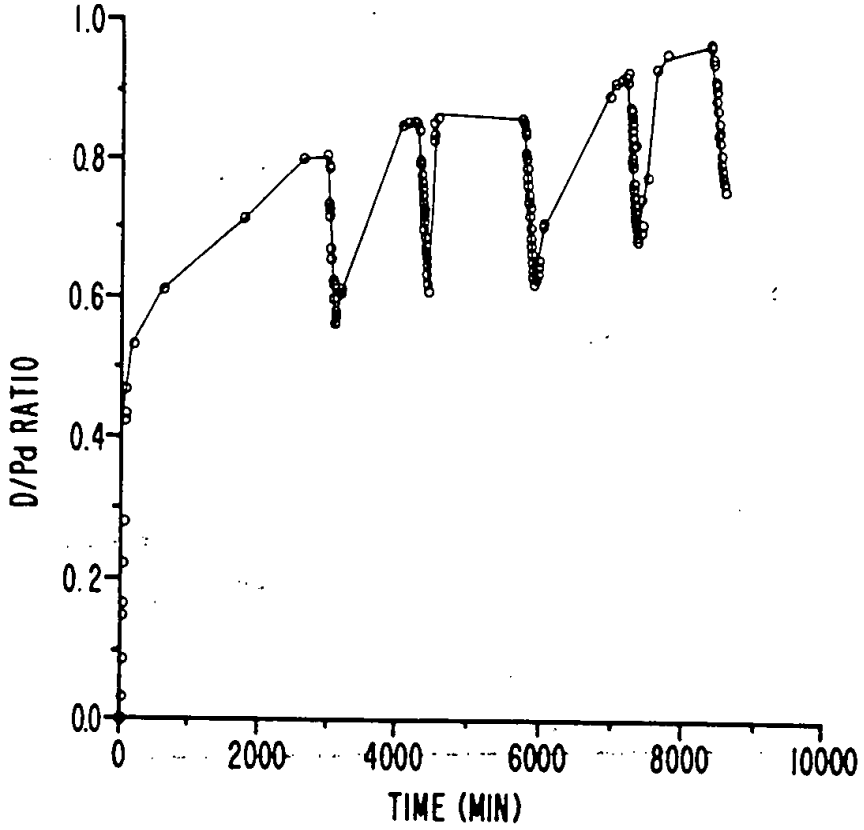
1.0
0.8
0.6
0.4
0.2
0.0
D/Pd RATIO
0
2000
4000
6000
8000
10000
TIME (MIN)

FIG. 7A

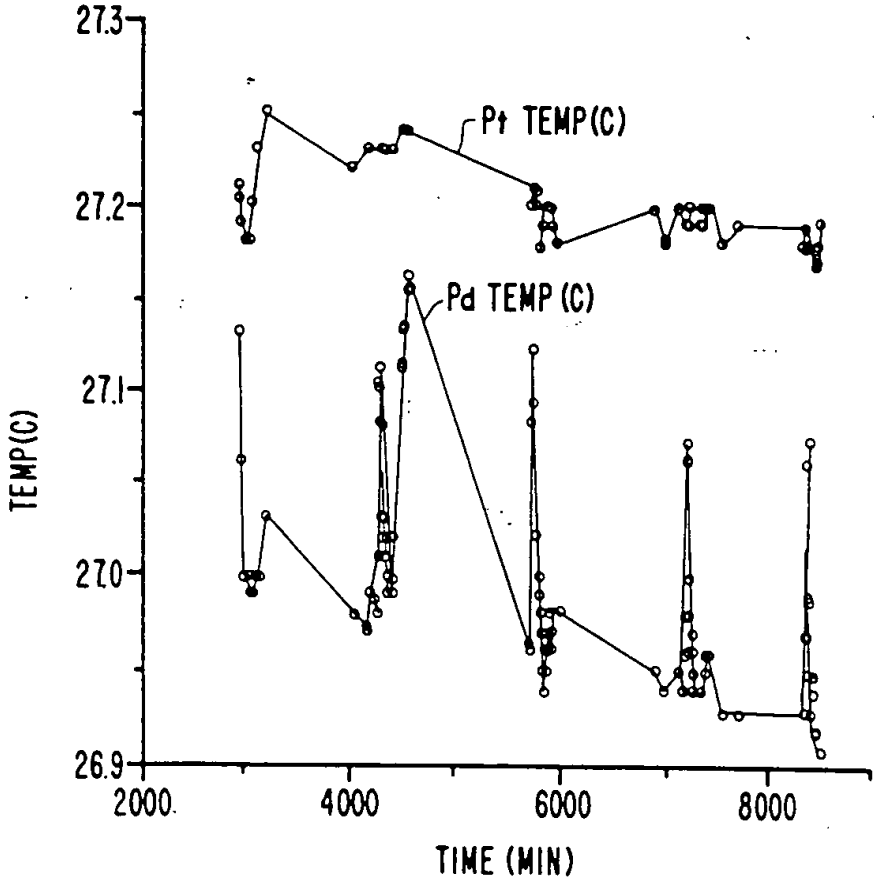
27.3
27.2
27.1
27.0
26.9
TEMP(C)
Pt TEMP(C)
Pd TEMP (C)
2000
4000
6000
8000
TIME (MIN)

FIG. 7B

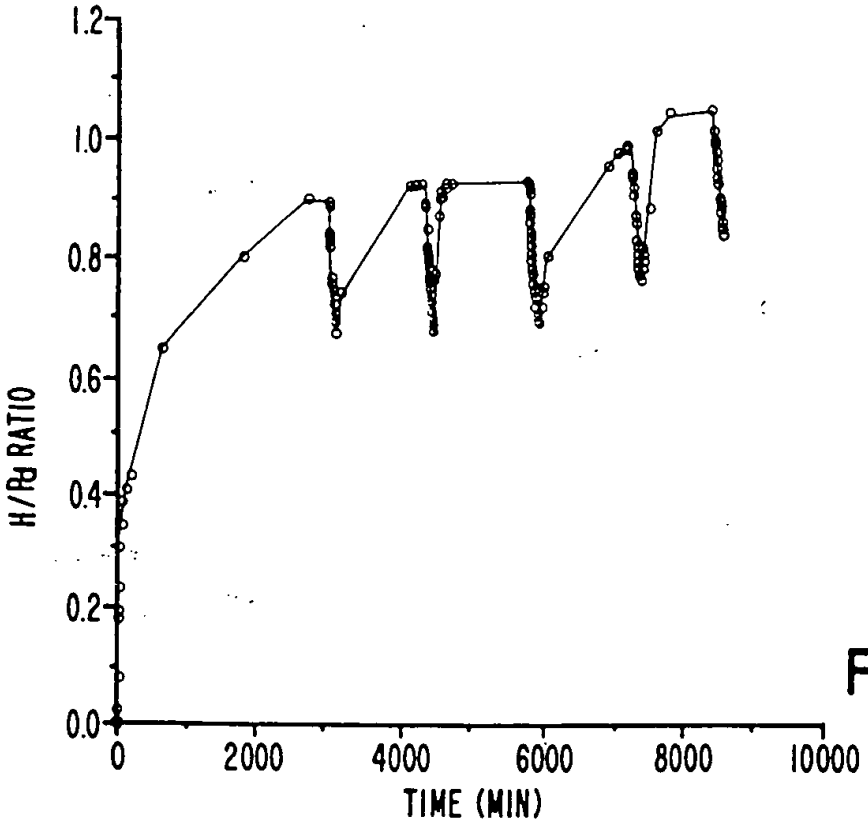
1.2
1.0
0.8
0.6
0.4
0.2
0.0
H/Pd RATIO
0
2000
4000
6000
8000
10000
TIME (MIN)

FIG. 8A

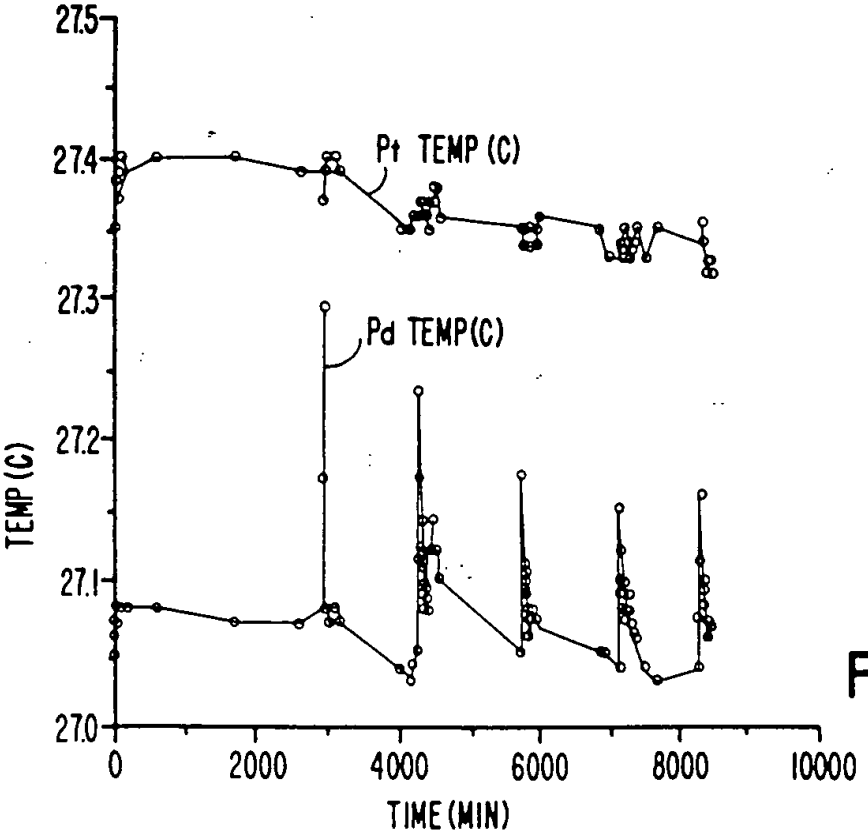
27.5
27.4
27.3
27.2
27.1
27.0
TEMP (C)
Pt TEMP (C)
Pd TEMP(C)
0
2000
4000
6000
8000
10000
TIME (MIN)

FIG. 8B

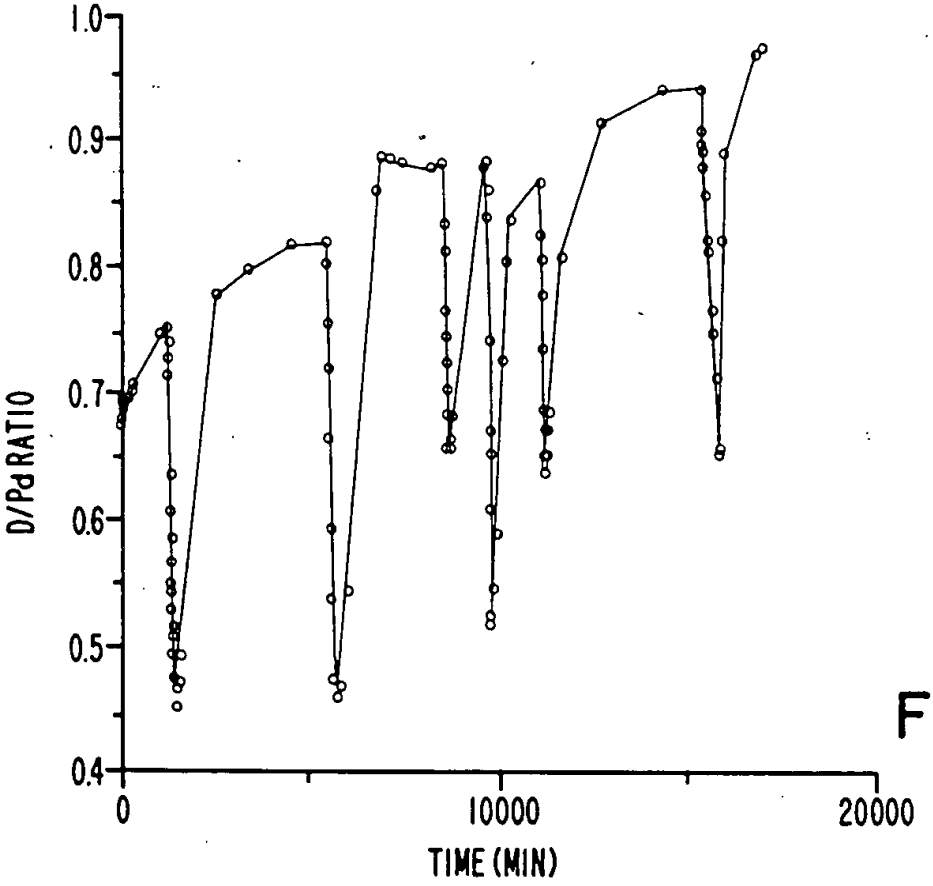
1.0
0.9
0.8
0.7
0.6
0.5
0.4
D/Pd RATIO
0
10000
20000
TIME (MIN)

FIG. 9A

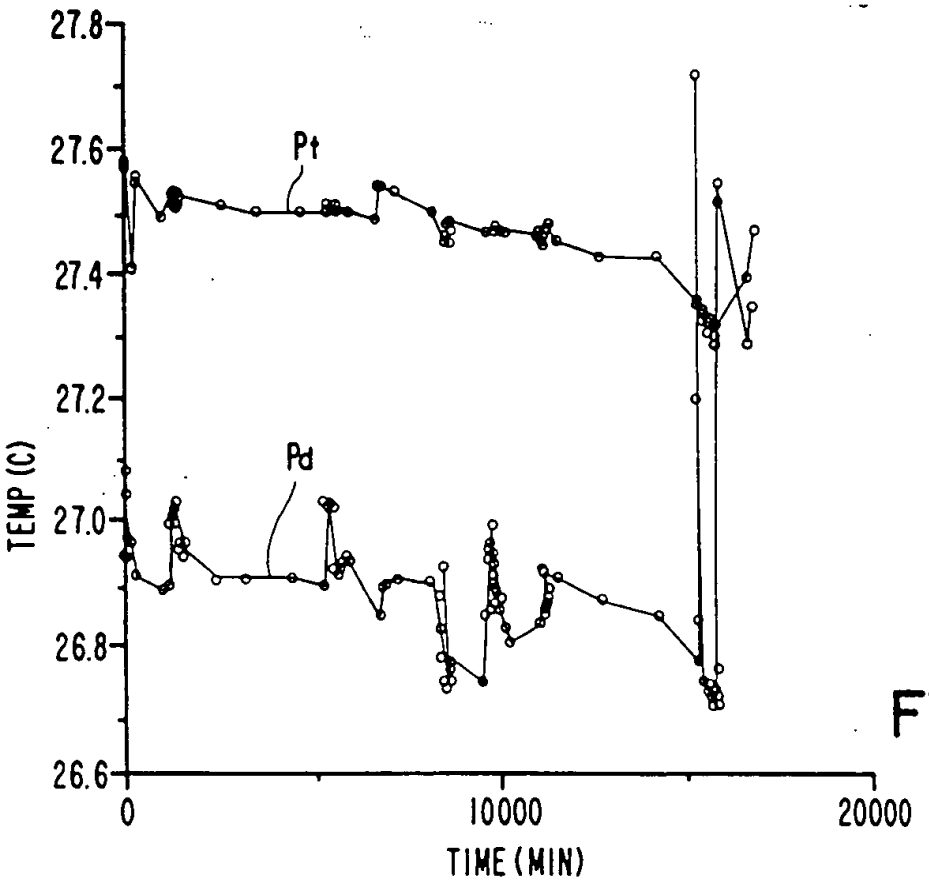
27.8
27.6
27.4
27.2
27.0
26.8
26.6
TEMP (C)
Pt
Pd
0
10000
20000
TIME (MIN)

FIG. 9B

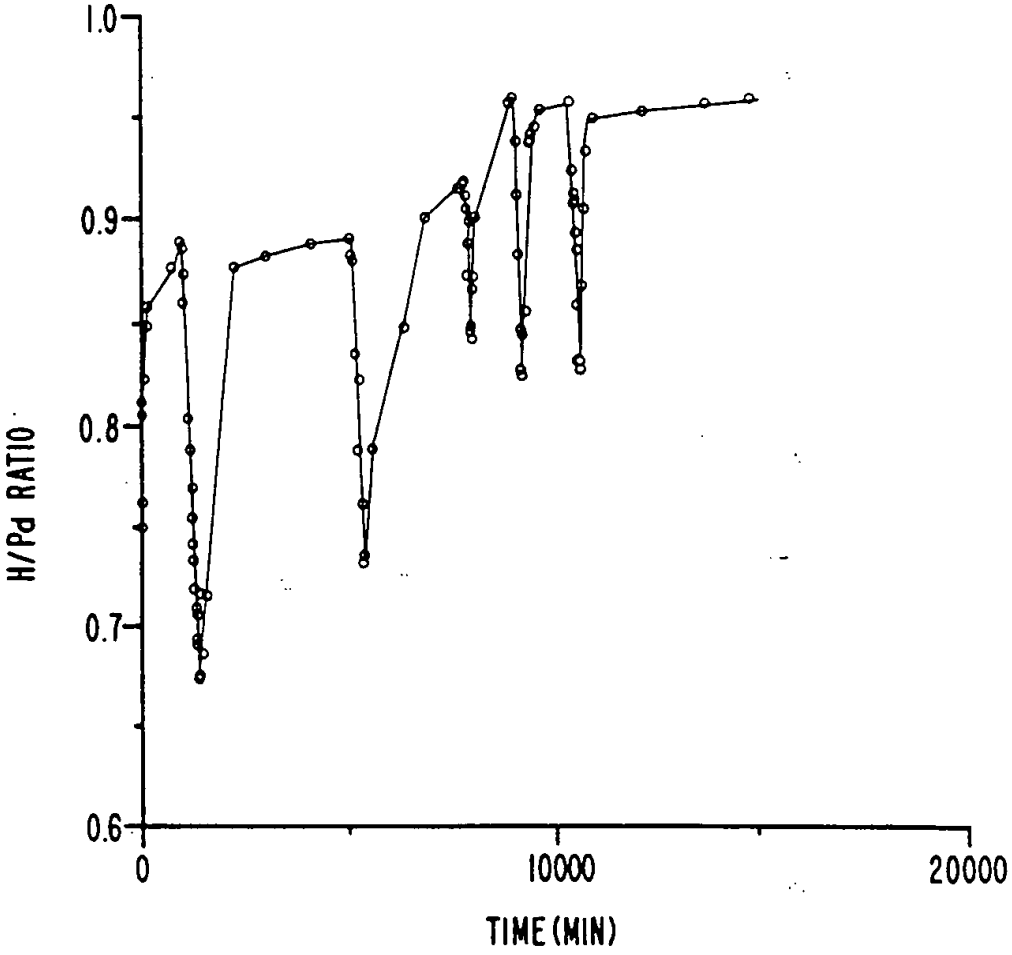

FIG. 9C

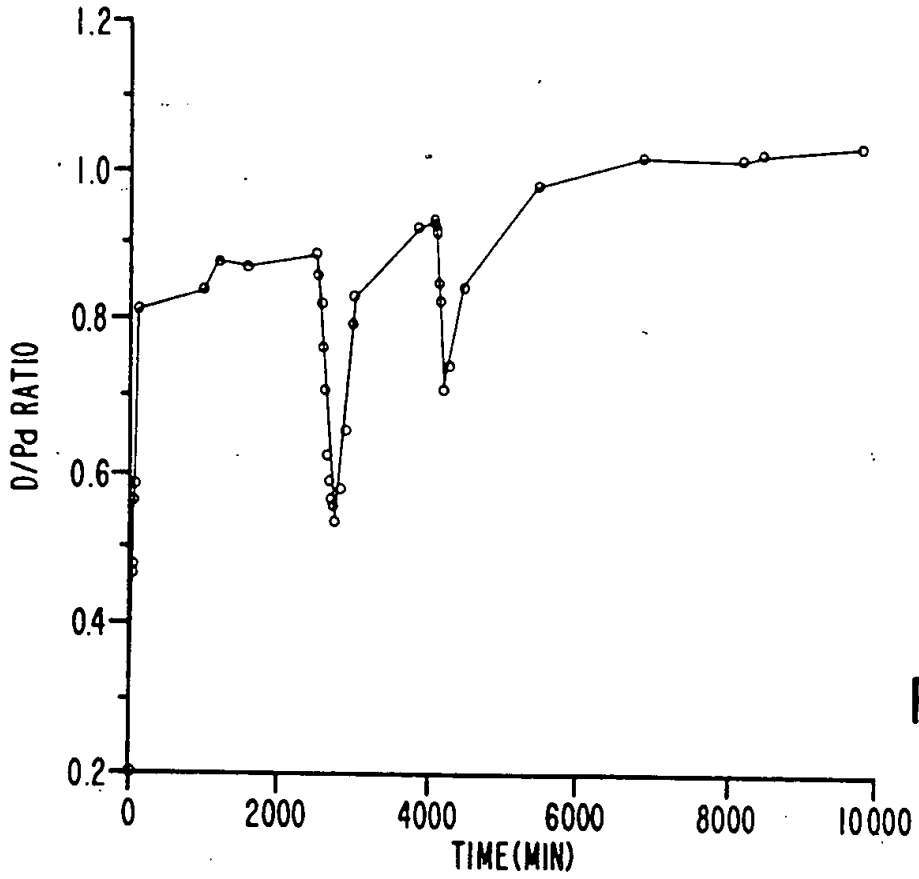
1.2
1.0
0.8
0.6
0.4
0.2
D/Pd RATIO
0
2000
4000
6000
8000
10000
TIME(MIN)

FIG. 9D

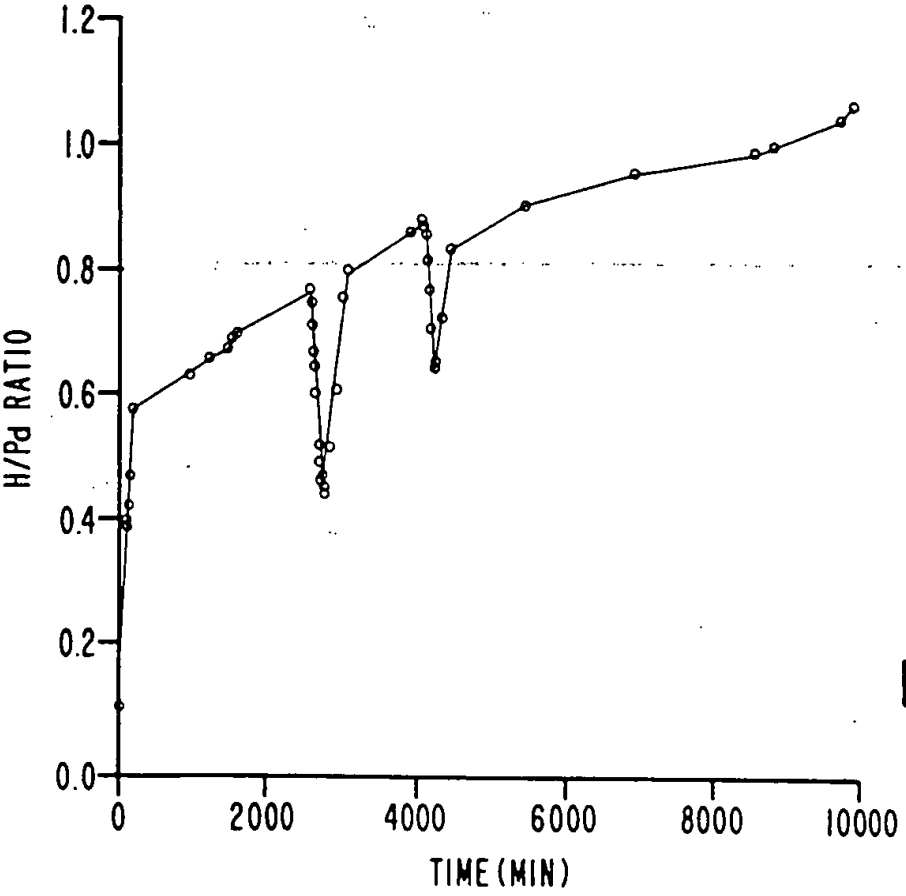
1.2
1.0
0.8
0.6
0.4
0.2
0.0
H/Pd RATIO
0
2000
4000
6000
8000
10000
TIME (MIN)

FIG. 9E

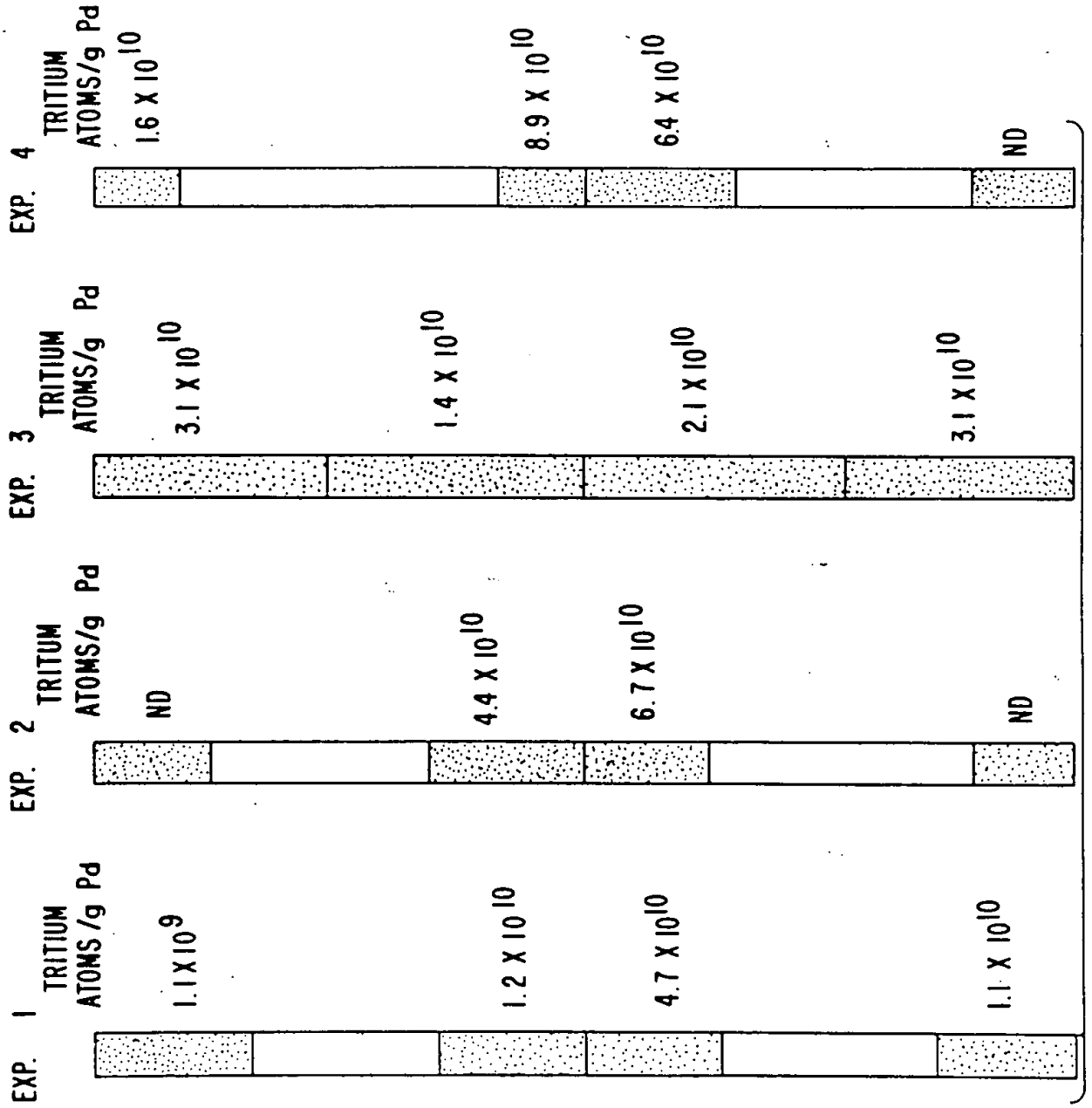
EXP. 1
TRITIUM ATOMS/g Pd
1.1 X 10^9
1.2 X 10^10
4.7 X 10^10
1.1 X 10^10
EXP. 2
TRITIUM ATOMS/g Pd
ND
4.4 X 10^10
6.7 X 10^10
ND
EXP. 3
TRITIUM ATOMS/g Pd
3.1 X 10^10
1.4 X 10^10
2.1 X 10^10
3.1 X 10^10
EXP. 4
TRITIUM ATOMS/g Pd
1.6 X 10^10
8.9 X 10^10
6.4 X 10^10
ND

FIG. 10

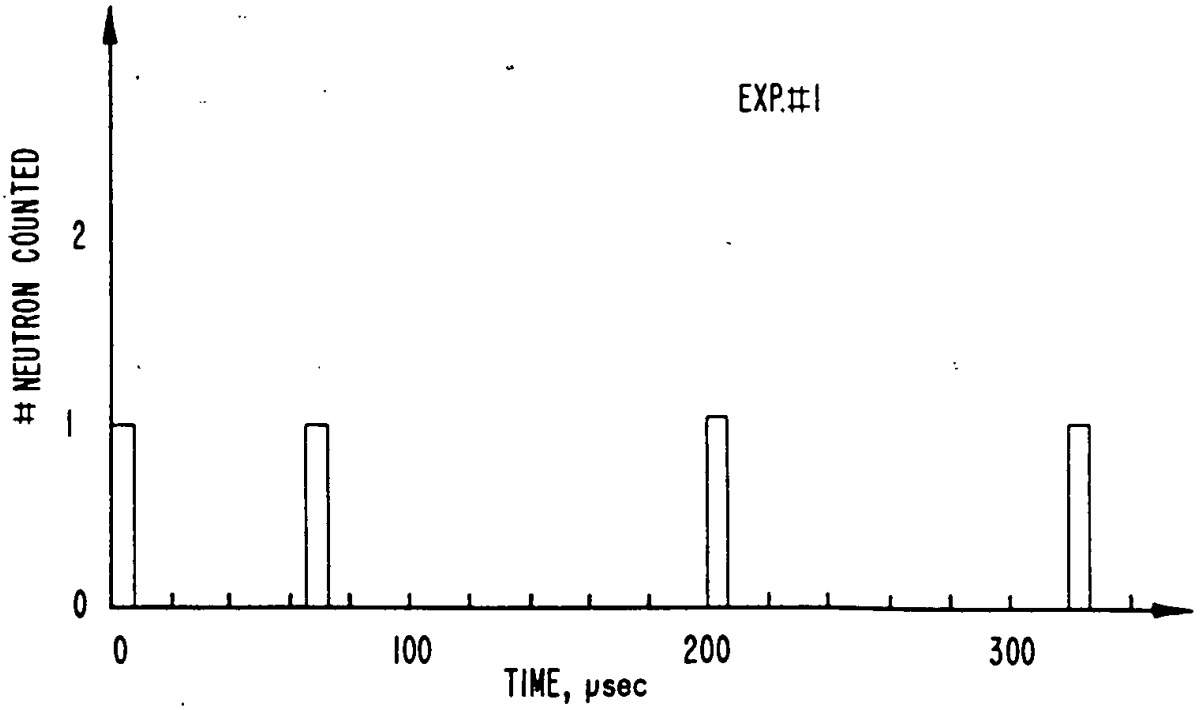

FIG. 11A

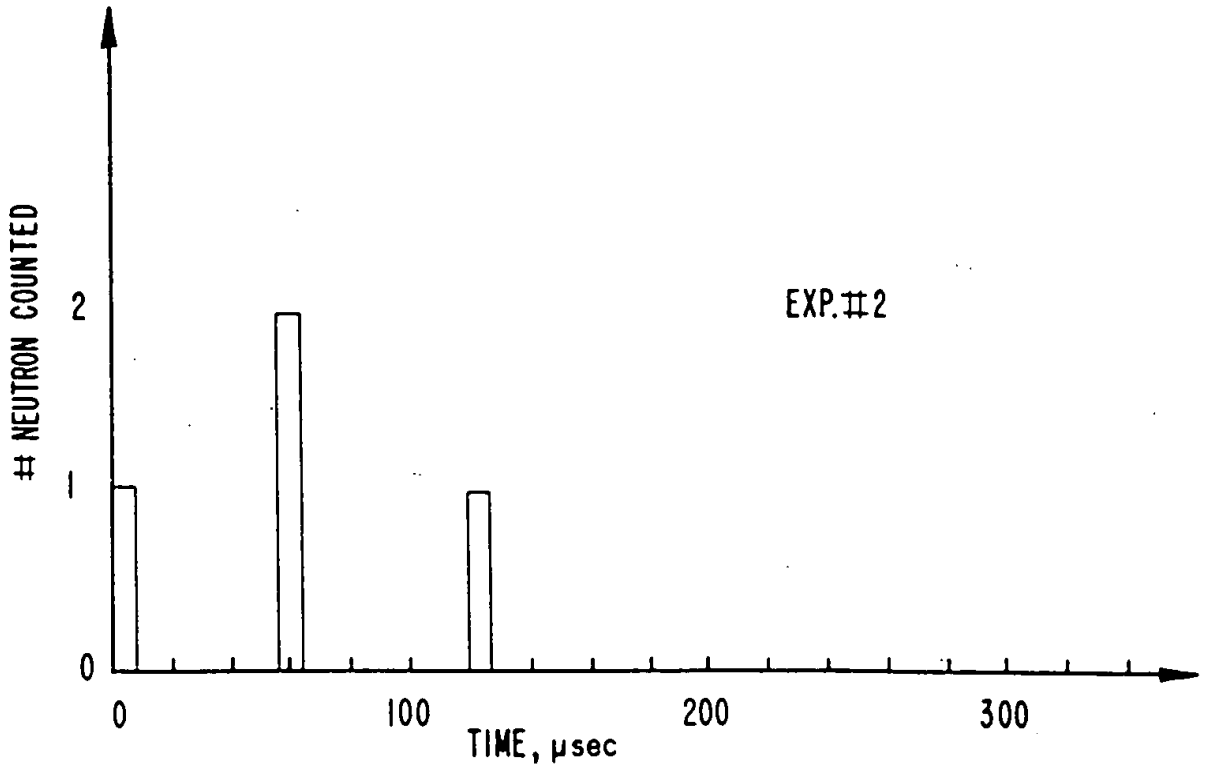

FIG. 11B

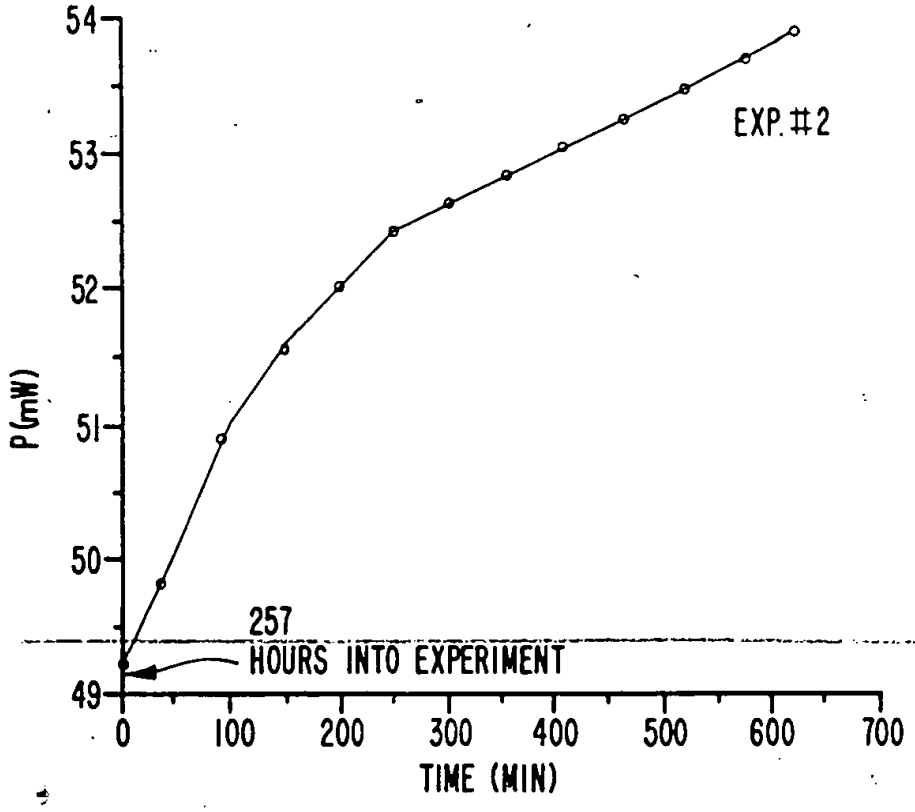

FIG. 12A

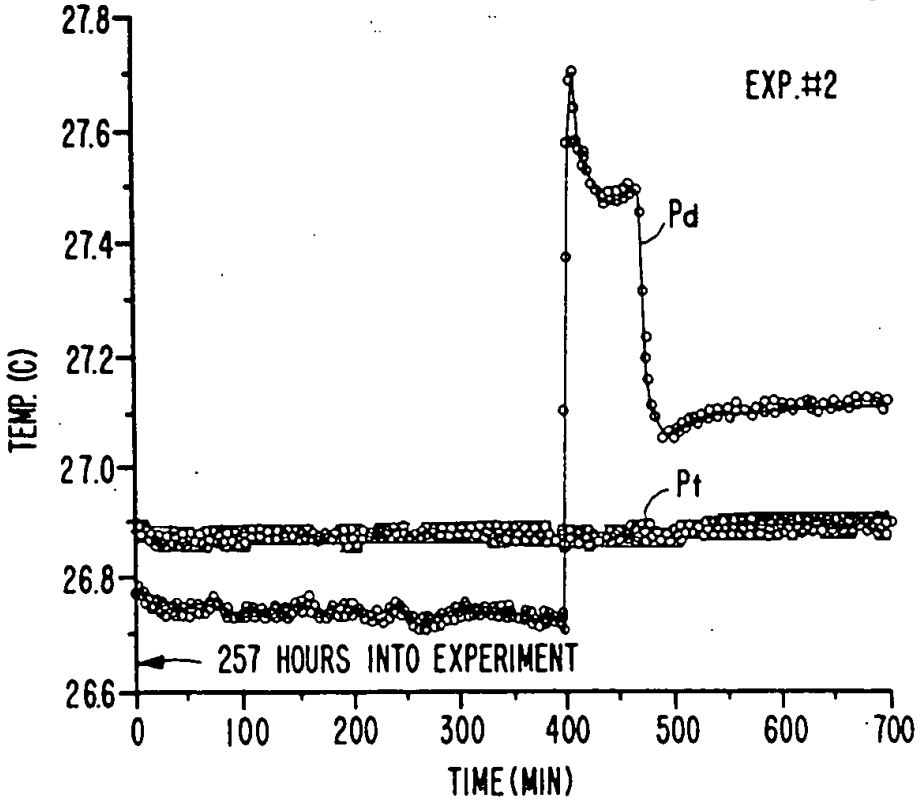

FIG. 12B

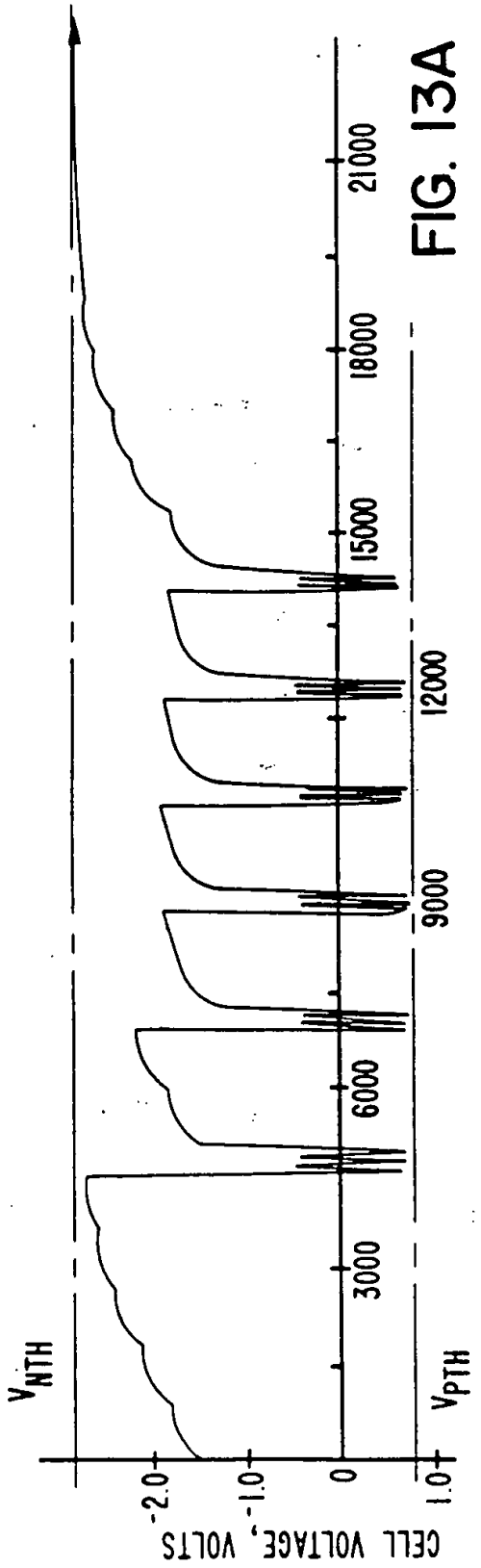

FIG. 13A

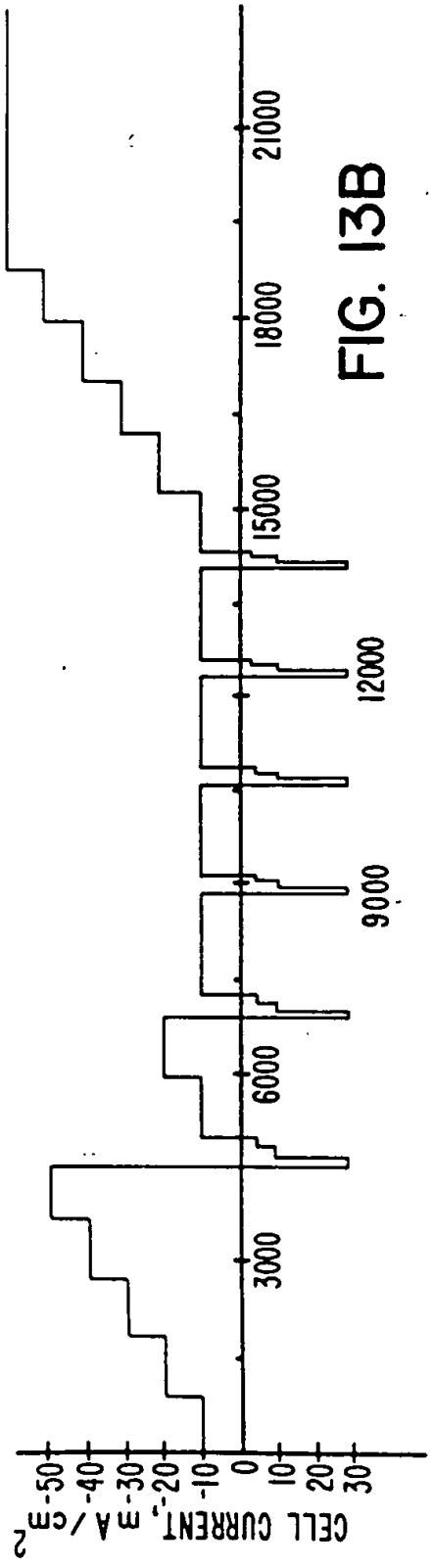

FIG. 13B

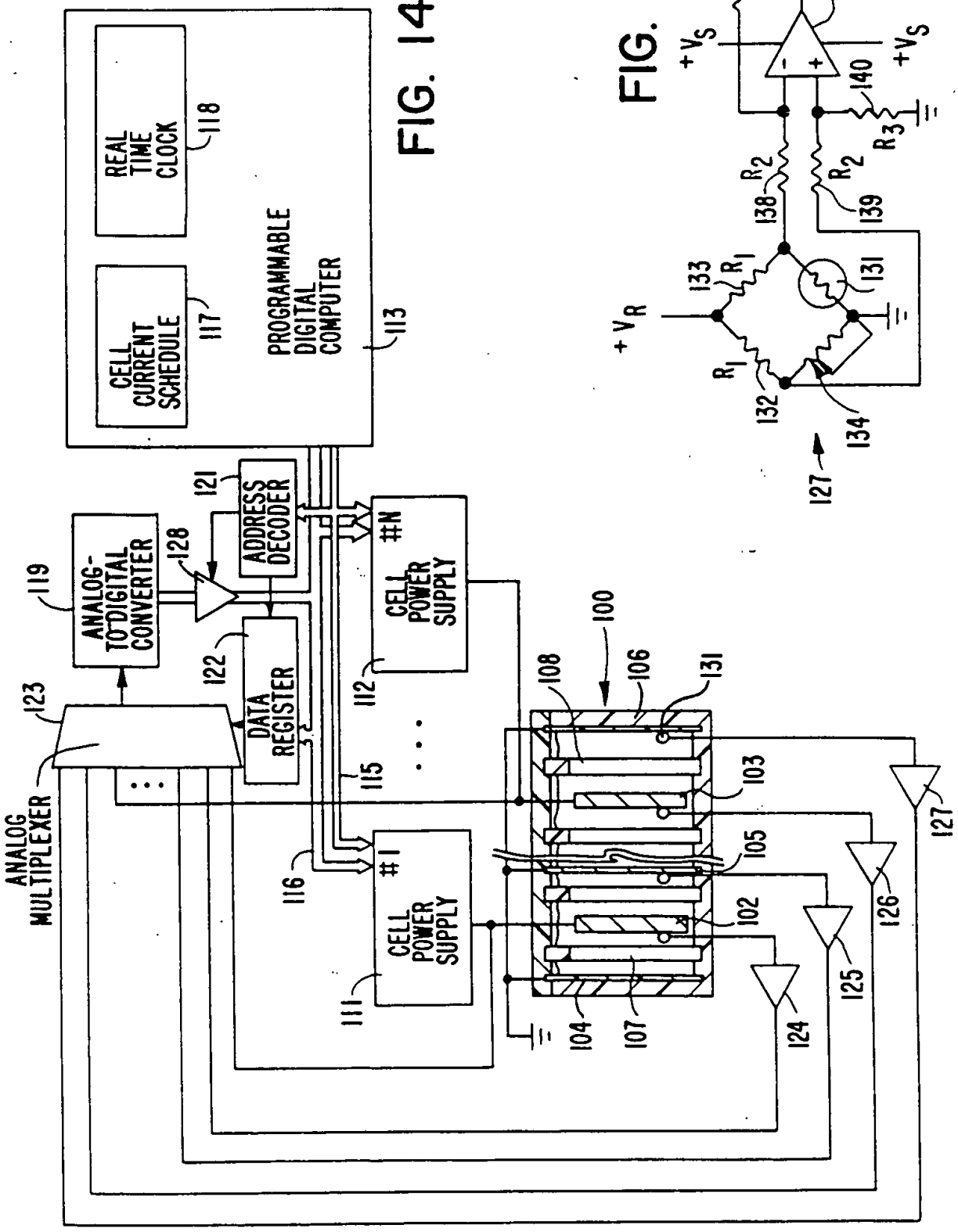
REAL TIME CLOCK
118
CELL CURRENT SCHEDULE
117
PROGRAMMABLE DIGITAL COMPUTER
113
121
ADDRESS DECODER
128
ANALOG-TO-DIGITAL CONVERTER
119
#N
CELL POWER SUPPLY
112
122
DATA REGISTER
123
ANALOG MULTIPLEXER
115
116
#1
CELL POWER SUPPLY
111
100
108
106
131
103
105
102
104
107
124
125
126
127

FIG. 14

V_O
R_3
141
135
$+V_S$
$-V_S$
140
R_3
R_2
R_2
138
139
133
R_1
131
$+V_R$
R_1
132
134
127

FIG. 15

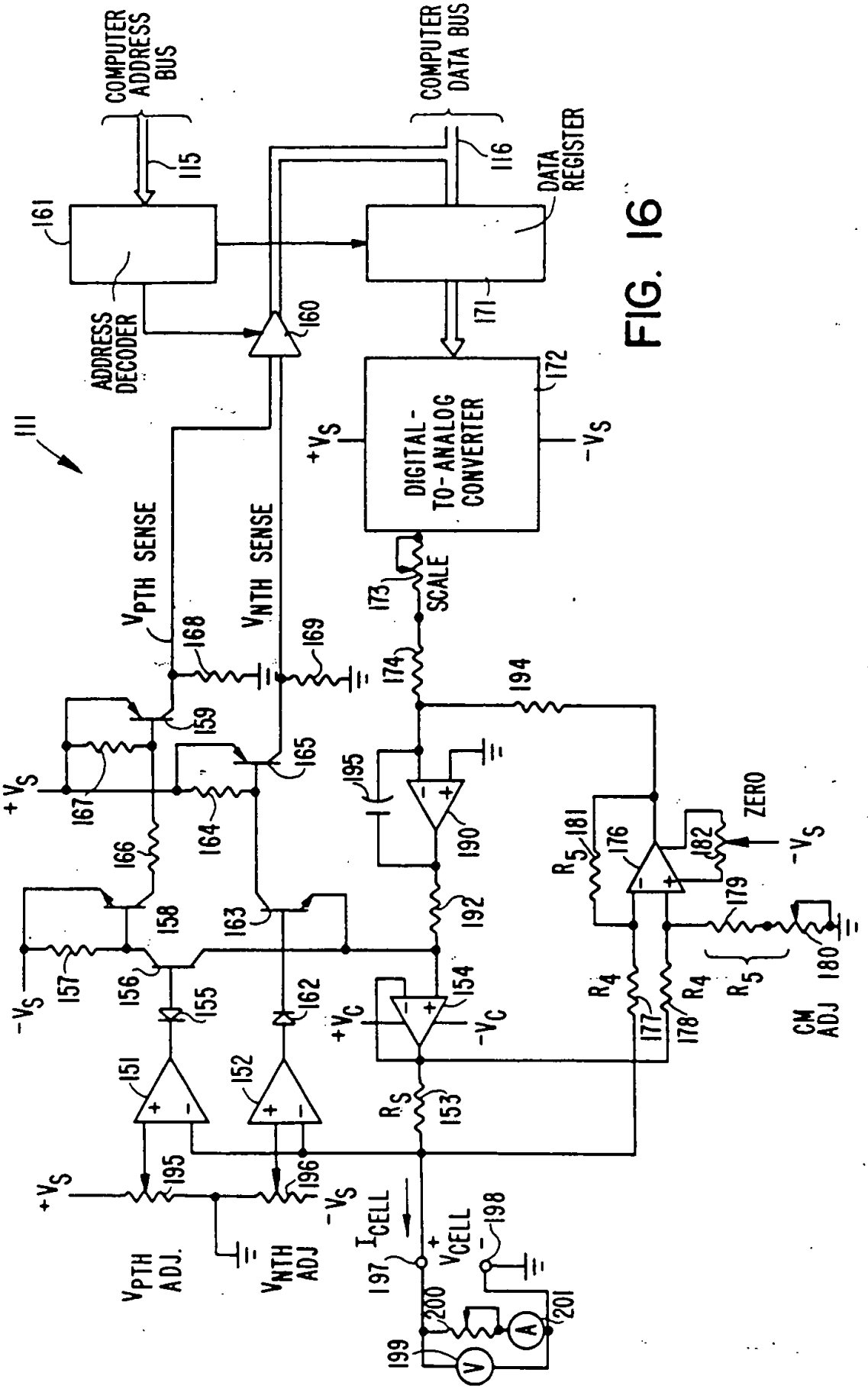
COMPUTER ADDRESS BUS
115
COMPUTER DATA BUS
116
DATA REGISTER
161
ADDRESS DECODER
160
171
172
DIGITAL-TO-ANALOG CONVERTER
+VS
-VS
111
VPTH SENSE
168
VNTH SENSE
169
173
SCALE
174
194
159
165
167
166
164
158
163
157
156
155
162
151
152
153
RS
154
+VC
-VC
195
190
192
R5
181
176
182
ZERO
179
R4
177
178
180
CM ADJ
196
VPTH ADJ.
VNTH ADJ
ICELL
VCELL
198
197
200
199
201
V
A

FIG. 16

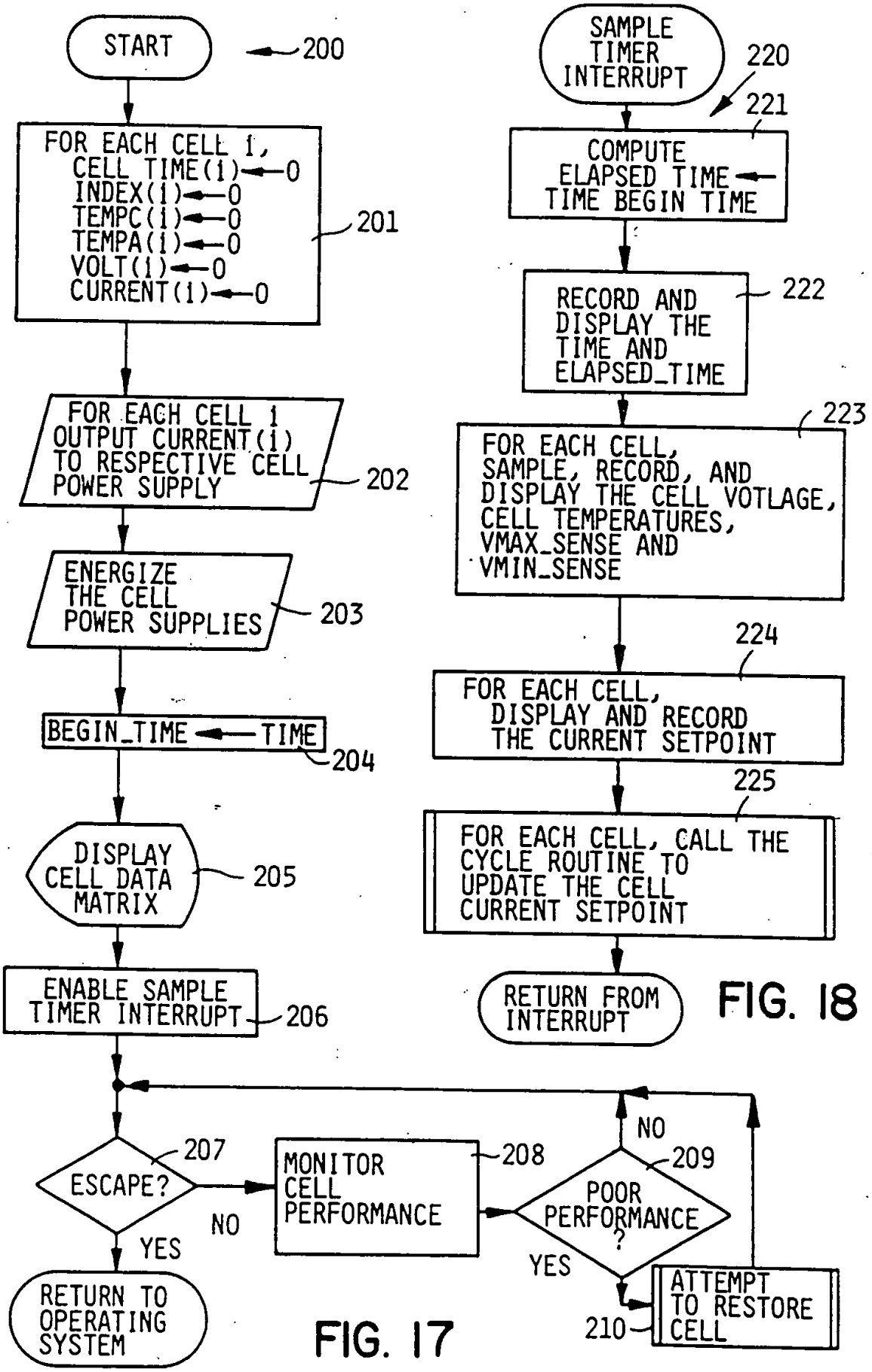
START
200
FOR EACH CELL i,
CELL TIME(i)←0
INDEX(i)←0
TEMPC(i)←0
TEMPA(i)←0
VOLT(i)←0
CURRENT(i)←0
201
FOR EACH CELL i
OUTPUT CURRENT(i)
TO RESPECTIVE CELL
POWER SUPPLY
202
ENERGIZE
THE CELL
POWER SUPPLIES
203
BEGIN_TIME←TIME
204
DISPLAY
CELL DATA
MATRIX
205
ENABLE SAMPLE
TIMER INTERRUPT
206
ESCAPE?
207
YES
NO
RETURN TO
OPERATING
SYSTEM
MONITOR
CELL
PERFORMANCE
208
POOR
PERFORMANCE
?
209
YES
NO
ATTEMPT
TO RESTORE
CELL
210
SAMPLE
TIMER
INTERRUPT
220
221
COMPUTE
ELAPSED TIME←
TIME BEGIN TIME
RECORD AND
DISPLAY THE
TIME AND
ELAPSED_TIME
222
FOR EACH CELL,
SAMPLE, RECORD, AND
DISPLAY THE CELL VOTLAGE,
CELL TEMPERATURES,
VMAX_SENSE AND
VMIN_SENSE
223
FOR EACH CELL,
DISPLAY AND RECORD
THE CURRENT SETPOINT
224
FOR EACH CELL, CALL THE
CYCLE ROUTINE TO
UPDATE THE CELL
CURRENT SETPOINT
225
RETURN FROM
INTERRUPT

FIG. 17

FIG. 18

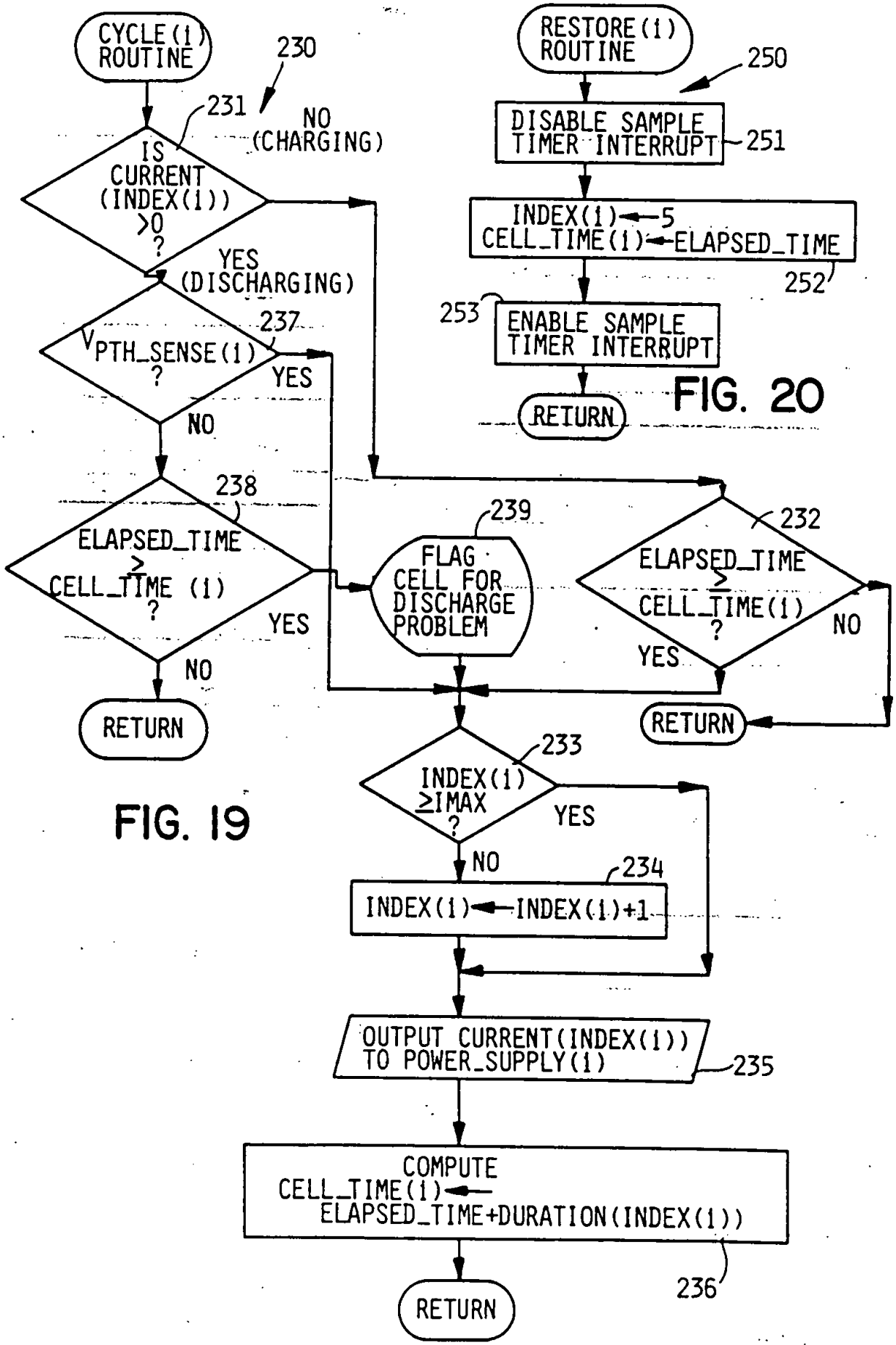
CYCLE(1) ROUTINE
230
231
IS CURRENT (INDEX(1)) >0 ?
NO (CHARGING)
YES (DISCHARGING)
237
VPTH_SENSE(1) ?
YES
NO
238
ELAPSED_TIME ≥ CELL_TIME (1) ?
YES
NO
RETURN
239
FLAG CELL FOR DISCHARGE PROBLEM
232
ELAPSED_TIME ≥ CELL_TIME(1) ?
NO
YES
RETURN
233
INDEX(1) ≥IMAX ?
YES
NO
234
INDEX(1)←INDEX(1)+1
OUTPUT CURRENT(INDEX(1)) TO POWER_SUPPLY(1)
235
COMPUTE CELL_TIME(1)← ELAPSED_TIME+DURATION(INDEX(1))
236
RETURN
RESTORE(1) ROUTINE
250
DISABLE SAMPLE TIMER INTERRUPT
251
INDEX(1)←5
CELL_TIME(1)←ELAPSED_TIME
252
253
ENABLE SAMPLE TIMER INTERRUPT
RETURN

FIG. 19

FIG. 20

A. CLASSIFICATION OF SUBJECT MATTER

IPC(5) : G21B 1/00

US CL :376/100

According to International Patent Classification (IPC) or to both national classification and IPC

B. FIELDS SEARCHED

Minimum documentation searched (classification system followed by classification symbols)

U.S. : 376/146; 204/129, 129.43, 228, 400, 402, DIG.6, DIG.9; 205/257, 265

Documentation searched other than minimum documentation to the extent that such documents are included in the fields searched

Electronic data base consulted during the international search (name of data base and, where practicable, search terms used)

C. DOCUMENTS CONSIDERED TO BE RELEVANT

Category*	Citation of document, with indication, where appropriate, of the relevant passages	Relevant to claim No.
X Y	Russian Journal of Physical Chemistry, vol. 34, No. 3, March 1960, Fedorova et al, pages 325,326.	1-3,7-11,14, 15,18,22,24, 25,28,29,31 4-6,12,13 16,17,19-21 23,26,27,30 32
Y	WO,A, 90/13897, (Drexler) 15 November 1990, (Note particularly page 8).	1-32
A	US,A, 4,663,006 (Yao et al) 05 May 1987.	

[X] Further documents are listed in the continuation of Box C. [ ] See patent family annex.

*	Special categories of cited documents:	"T"	later document published after the international filing date or priority date and not in conflict with the application but cited to understand the principle or theory underlying the invention
"A"	document defining the general state of the art which is not considered to be part of particular relevance	"X"	document of particular relevance; the claimed invention cannot be considered novel or cannot be considered to involve an inventive step when the document is taken alone
"E"	earlier document published on or after the international filing date	"Y"	document of particular relevance; the claimed invention cannot be considered to involve an inventive step when the document is combined with one or more other such documents, such combination being obvious to a person skilled in the art
"L"	document which may throw doubts on priority claim(s) or which is cited to establish the publication date of another citation or other special reason (as specified)	"&"	document member of the same patent family
"O"	document referring to an oral disclosure, use, exhibition or other means		
"P"	document published prior to the international filing date but later than the priority date claimed		

Date of the actual completion of the international search 17 SEPTEMBER 1992	Date of mailing of the international search report 12 NOV 1992
Name and mailing address of the ISA/ Commissioner of Patents and Trademarks Box PCT Washington, D.C. 20231 Facsimile No. NOT APPLICABLE	Authorized officer HARVEY E. BEHREND Telephone No. (703) 308-0439

Form PCT/ISA/210 (second sheet)(July 1992)*

C (Continuation). DOCUMENTS CONSIDERED TO BE RELEVANT

Category*	Citation of document, with indication, where appropriate, of the relevant passages	Relevant to claim No.
X Y	Transactions of the Faraday Society, vol. 55, Part 8, No. 440, August 1959, Flanagan et al, pages 1400-1408 (Note particularly pages 1401,1403,1404).	1-3,7,9 10,11,15, 22,24,25, 26,29 4-6,8, 12-14, 16-21,23, 27,28,30-32
X Y L	Nature, vol. 342, 23 November 1989, Williams et al., pages 375-384 (Note particularly the bottom of pages 381) (also cited as casting douby on obtaining nuclear fusion by forcing deuterium into a hydrogen absorbing material).	1-3,7,9-11, 15,22,24, 25,29 4-6,8,12-14, 16-21,23,26- 28,30-32 1-32
Y.	Can. J. Chem., vol. 37, (1959), Schuldiner et al, pages 228-237 (Note particularly page 229).	4-6,12,13, 16,17,19-21 23,30
Y	WO,A, 91/03055 (Wadsworth et al) 07 March 1991.	1-32
A	US,A, 3,113,080 (Andrus) 03 December 1963 (Note particularly col. 5 lines 8+).	
Y	J. Electroanal Chem., vol. 39, (1972) Dandapani et al., pages 323-332.	1-32
A	US,A, 2,139,529 (Streicher) 06 December 1938.	
L	Nature, vol. 340, 17 August 1989, Lewis et al, pages 525-530 (Note particularly col. 2 on page 525) (cited as casting doubt on obtaining nuclear fusion by forcing deuterium into a hydrogen absorbing material.	1-32
A	US,A, 3,520,788 (Paehr) 14 July 1970.	
A	US,A, 2,451,340 (Jernstedt) 12 October 1948.	
Y	US,A, 3,300,345 (Lyons, Jr.) 24 January 1967.	11-13,29
L	J. of Fusion Energy, vol. 9, No. 3, (1990, Myers et al, pages 263-268 (cited as coating doubt on obtaining nuclear fusion by forcing deuterium into a hydrogen absorbing material).	1-32